

This work was written as part of one of the author's official duties as an Employee of the United States Government and is therefore a work of the United States Government. In accordance with 17 U.S.C. 105, no copyright protection is available for such works under U.S. Law.

Public Domain Mark 1.0

<https://creativecommons.org/publicdomain/mark/1.0/>

Access to this work was provided by the University of Maryland, Baltimore County (UMBC) ScholarWorks@UMBC digital repository on the Maryland Shared Open Access (MD-SOAR) platform.

Please provide feedback

Please support the ScholarWorks@UMBC repository by emailing scholarworks-group@umbc.edu and telling us what having access to this work means to you and why it's important to you. Thank you.

An Examination of the Recent Stability of Ozonesonde Global Network Data

Date Updated: 30 August 2022

Ryan M. Stauffer¹, Anne M. Thompson^{2,1}, Debra E. Kollonige^{3,1}, David W. Tarasick⁴, Roeland Van Malderen⁵, Herman G. J. Smit⁶, Holger Vömel⁷, Gary A. Morris⁸, Bryan J. Johnson⁸, Patrick D. Cullis^{9,8}, Rene Stübi¹⁰, Jonathan Davies⁴, and Michael M. Yan^{11,1}

¹Atmospheric Chemistry and Dynamics Laboratory, NASA/GSFC, Greenbelt, MD, USA

²Joint Center for Earth Systems Technology, University of Maryland Baltimore County, Baltimore, MD, USA

³Science Systems and Applications, Inc., Lanham, MD, USA

⁴Environment and Climate Change Canada, Downsview, ON, CA

⁵Royal Meteorological Institute of Belgium, Uccle (Brussels), Belgium

⁶Institute for Energy and Climate Research: Troposphere (IEK8), Jülich Research Centre, Jülich, Germany

⁷National Center for Atmospheric Research Earth Observations Laboratory, Boulder, CO, USA

⁸Global Monitoring Laboratory, NOAA Earth System Research Laboratory, Boulder, CO, USA

⁹Cooperative Institute for Research in Environmental Sciences, University of Colorado, Boulder, CO, USA

¹⁰Federal Office of Meteorology and Climatology, MeteoSwiss, Aerological Station, Payerne, Switzerland

¹¹Kellogg Brown & Root, Fulton, MD, USA

Corresponding author: Ryan M. Stauffer (ryan.m.stauffer@nasa.gov)

Key Points:

- Global ozonesonde total column ozone stability averages $\sim \pm 2\%$ relative to measurements from multiple satellite instruments since 2004
- A sudden ozonesonde low bias affects a subset of stations using one manufacturer, and is mostly confined to the tropics
- Continuous evaluation of ozonesonde data against independent measurements will facilitate ongoing monitoring of the stability of the data

Keywords: Ozonesonde, Data Quality Assurance, Satellite Ozone, Ozone Trends

Index Terms: 0340, 0394, 0365

This article has been accepted for publication and undergone full peer review but has not been through the copyediting, typesetting, pagination and proofreading process, which may lead to differences between this version and the [Version of Record](#). Please cite this article as [doi: 10.1029/2022EA002459](https://doi.org/10.1029/2022EA002459).

This article is protected by copyright. All rights reserved.

Abstract

The recent Assessment of Standard Operating Procedures for OzoneSondes (ASOPOS 2.0; WMO/GAW Report #268) addressed questions of homogeneity and long-term stability in global electrochemical concentration cell (ECC) ozone sounding network time series. Among its recommendations was adoption of a standard for evaluating data quality in ozonesonde time-series. Total column ozone (TCO) derived from the sondes compared to TCO from Aura's Ozone Monitoring Instrument (OMI) is a primary quality indicator. Comparisons of sonde ozone with Aura's Microwave Limb Sounder (MLS) are used to assess the stability of stratospheric ozone. This paper provides a comprehensive examination of global ozonesonde network data stability and accuracy since 2004 in light of the sudden post-2013 TCO "dropoff" of ~3-4% that was reported previously at select stations (Stauffer et al., 2020). Comparisons with Aura OMI TCO averaged across the network of 60 stations are stable within about $\pm 2\%$ over the past 18 years. Sonde TCO has similar stability compared to three other TCO satellite instruments, and the stratospheric ozone measurements average to within $\pm 5\%$ of MLS from 50 to 10 hPa. Thus, sonde data are reliable for trends, but with a caveat applied for a subset of dropoff stations in the tropics and subtropics. The dropoff is associated with only one of two major ECC instrument types. A detailed examination of ECC serial numbers pinpoints the timing of the dropoff. However, we find that overall, ozonesonde data are stable and accurate compared to independent measurements over the past two decades.

Plain Language Summary

Ozonesondes provide accurate ozone measurements from the surface to ~30 km altitude and are used as a reference for studies of satellite data, trends, pollution and climate. Updated

guidelines for sonde preparation and adoption of sonde total column ozone (TCO) comparisons with satellite TCO as a “data quality” reference were published in 2021 by the ASOPOS (Assessment of Standard Operating Procedures for OzoneSondes) 2.0 panel in WMO/GAW Report 268. We report the first application of the ASOPOS 2.0 protocol to TCO evaluation from the 60-station global ozonesonde network (42,042 profiles total). With Aura OMI TCO as the satellite reference (Oct. 2004 to mid-2021), we find that TCO readings from the global ozonesonde network are remarkably stable, consistently within $\pm 2\%$ of the satellite. An exception occurs at only a small subset of tropical and subtropical locations that use one type of ozonesonde instrument. The latter result confirms our earlier report that a sudden TCO drop occurs at selected sites after 2013. The timing and magnitude of the dropoff are revisited. The hypothesis that ozonesonde production changes are a contributor remains, with station-specific factors possibly affecting the magnitude of the bias. Overall, global ozonesonde network data are of high quality and stability.

1 ECC Ozonesondes and Data Quality Assurance

1.1 The ECC Ozonesonde and Evaluations of Its Data Quality

The electrochemical concentration cell (ECC) ozonesonde, versions of which have existed since the 1960s (**Komhyr, 1969; Komhyr and Harris, 1971; Komhyr 1986**), are expendable, balloon-borne instruments that serve a vital role in global atmospheric ozone monitoring. Always paired with a meteorological radiosonde, the ECC provides continuous, high-quality, in-situ measurements of ozone with high vertical resolution (100-150 m) from the surface to over 30 km altitude, characteristics that no other instrument, remote-sensing or otherwise, can match. The measurement principle of the ECC is based on the wet chemical reaction of ozone in a neutral-buffered potassium iodide (KI) solution, such that approximately two electrons flow in an external circuit in the ECC for each ozone molecule absorbed into the solution (**Smit, Thompson, and ASOPOS 2.0, 2021; Tarasick et al., 2021**). The magnitude of the resulting current is transmitted via the radiosonde to a receiving station and converted into ozone partial pressure. ECC ozonesondes are currently launched at over 50 stations around the globe with regularity (**Smit, Thompson, and ASOPOS 2.0, 2021**), forming the global ozonesonde network. The data are used for satellite and model evaluation (**Hubert et al., 2016; Stauffer et al., 2019**), developing ozone climatologies (**Tilmes et al., 2012; Liu et al., 2013a,b; Hassler et al., 2018; Stauffer et al., 2018**), pollution and climate studies (**Logan et al., 2003; Witte et al., 2008; Cooper et al., 2010; Moeini et al., 2020**), and calculating ozone trends (**Logan et al., 1999; WMO, 2018; Petropavlovskikh et al., 2019; Thompson et al., 2021**). Ozonesondes produced by one of two ECC manufacturers are operated at nearly all global network stations: Environmental Science (EnSci; currently Z model; Westminster, CO, USA) and Science Pump Corporation (SPC; currently 6A model; Camden, NJ, USA).

Over the past 25+ years, significant effort has been invested to increase our understanding of ECC measurements and the factors affecting their uncertainty. Instrument performance has been evaluated through laboratory experiments (**Smit et al., 2007; Smit and ASOPOS, 2014; Thompson et al., 2019; Smit, Thompson, and ASOPOS 2.0, 2021**), field campaigns (**Komhyr et al., 1995; Boyd et al., 1998; Deshler et al., 2008**), and analysis of historical records (**Tarasick et al., 2019**). Uncertainties associated with ECC ozonesonde measurements have decreased from >10% in the late 1990s, to near 5% today (**Witte et al., 2018; Tarasick et al., 2021; Smit, Thompson, and ASOPOS 2.0, 2021**). The satellite instrument community has requested even more stable and reliable data to detect and quantify drift in satellite measurements that span a decade or more (**Hubert et al., 2016**).

Laboratory tests include the series of Jülich OzoneSonde Intercomparison Experiments (JOSIE; **Smit and Kley, 1998; Smit and Straeter, 2004; Smit et al., 2007; Thompson et al., 2019**), held at the World Calibration Centre for OzoneSondes (WCCOS) in Jülich, Germany. In the JOSIE experiments, ozonesondes are placed in the WCCOS environmental chamber and compared to a reference UV ozone photometer (OPM) during simulated atmospheric soundings (**Profitt and McLaughlin, 1983**; the OPM was also flown in the field experiment described in **Deshler et al., 2008**). The JOSIE experiments have examined the varying performance among ECC (and other ozonesonde type) manufacturers, multiple KI sensing solution types (SSTs) employed in the network, and the parameters used in the equation to convert the raw ozonesonde cell current to ozone partial pressure, e.g., pump efficiency (**Johnson et al., 2002**) and temperature, “background” current (**Thornton and Niaz, 1982; Reid et al., 1996; Vömel and Diaz, 2010; Newton et al., 2016**), ozone absorption (**Davies et al., 2003**) and conversion efficiency, and time response of the cell (**Johnson et al., 2002; Vömel et al., 2020**).

The results from the JOSIE experiments led to the formulation of ozonesonde standard operating and data processing procedures by the Assessment of Standard Operating Procedures for OzoneSondes Panel (ASOPOS; **Smit and ASOPOS, 2012; Deshler et al., 2017**). The data processing techniques devised by ASOPOS led to a common method by which a station's ozonesonde data record can be "homogenized". Homogenization accounts for changes in instrumentation, SST, preparation procedures, and other factors, and reduces or eliminates artifacts which may otherwise appear as step changes in the ozonesonde time series.

Homogenized ozonesonde data show better agreement with independent ozone measurements compared to the non-homogenized versions (**Tarasick et al., 2016; Van Malderen et al., 2016; Witte et al., 2017; Thompson et al., 2017; Sterling et al., 2018; Witte et al., 2019; Ancellet et al., 2022**). The most recent report on ozonesonde measurement principles and best-practices was published in mid-2021 by the ASOPOS 2.0 Panel (**Smit, Thompson, and ASOPOS 2.0, 2021**).

1.2 Data Quality Indicators for Ozonesonde Measurements

One of the most significant advances in the ASOPOS 2.0 Report was the adoption of stronger recommendations for assessing ozonesonde data quality across the global network. Although co-located ground-based instruments are a logical first choice for evaluating the quality of soundings at individual sites (e.g., **Sterling et al., 2018; Witte et al., 2019**), not all stations have such an instrument, usually a Dobson, Brewer or SAOZ. Furthermore, ground-based instruments must themselves be calibrated with global standards and the frequency of calibration varies from site to site. Thus, with the emergence of high-quality, consistently calibrated, and regularly updated satellite ozone measurements over the past two to three decades, providers of ozonesonde data typically compare their integrated total column ozone (TCO) amounts with satellite overpass measurements. Improved agreement of reprocessed sonde data with satellite

TCO has been a major criterion for evaluating the success of homogenization in the studies cited above.

Given the longevity and coordinated calibration of the NASA and NOAA UV-based satellite instruments, ASOPOS 2.0 recommends that Aura's Ozone Monitoring Instrument (OMI) be used to assess global data quality in sondes after 2004 (Chapter 5 in **Smit, Thompson, and ASOPOS 2.0, 2021**). For example, the post-2013 ozonesonde TCO "dropoff", first noted at Costa Rica in reprocessed SHADOZ data (**Thompson et al., 2017**) and at several NOAA stations (**Sterling et al., 2018**) was identified with OMI comparisons. Likewise, with Aura's Microwave Limb Sounder (MLS) giving very stable ozone measurements for 18 years, ASOPOS 2.0 recommends the use of MLS profiles to track data quality in the stratospheric segment of the sondes. Thus, using a combination of OMI and MLS from 2004-2019, **Stauffer et al. (2020;** "S20" hereafter) were able to demonstrate that most of the unexpected low ozone at ~1/3 of 37 stations worldwide is due to anomalous apparent losses in the lower and middle stratosphere. Other than at the Hilo and Costa Rica stations, no systematic low bias in tropospheric measurements was found. The anomalously low tropospheric ozone found at those two stations may or may not be related to the TCO drop. Several potential sources of the bias, including the radiosondes paired with the ozonesondes and radiosonde pressure offsets (**Steinbrecht et al., 2008; Stauffer et al., 2014; Inai et al., 2015**) were ruled out. The TCO drop appeared only at stations launching the EnSci ECC. Manufacturing changes in the EnSci ECC were suspected as a contributor, as an analysis of serial numbers (S/Ns) revealed that the sudden drop and a consistent low ozone bias began approximately with S/N 25000 (~2013-2014, depending on station) when considering all affected stations.

Since the revelation that significant portions of the global network appear to be affected by this problem, ASOPOS 2.0 formed a Task Team to more closely examine the TCO drop and expand the analysis to additional ozonesonde stations. Efforts have been focused on metadata gathering, additional laboratory and field tests, and enhanced data analysis, the last of which is the subject of this paper. Our intentions are: (1) to provide the community with an update on the current state of the stability and quality of ozonesonde data in the global network, and (2) better characterize the TCO drop throughout the global network.

This study is the first application of the ASOPOS 2.0 recommendations for data quality evaluation to data collected from the global ozonesonde network since 2004. Measurements are taken from 60 stations for which data are publicly available. We extend the records of the 37 stations analyzed in S20 and feature more homogenized data than the earlier study. The paper is organized as follows: Section 2 describes the data sets and methods used to assess the global ozonesonde network data; Section 3 presents the time series of ozonesonde and satellite comparisons for the network in various latitude bands, and a detailed analysis of EnSci S/Ns to better pinpoint the timing of the dropoff and quantify the resulting step change in ozone. We also discuss the next steps that the ASOPOS Task Team will pursue to solve the TCO drop. Section 4 is a summary, and advocates standard operating procedures to monitor the future stability of network data against changes to instrumentation or preparation procedures, and to quantify the effects of ozonesonde data homogenization.

2 Data and Methods

We employ satellite data as our primary reference to evaluate global ozonesonde network data because independent ground-based TCO data are unavailable at some stations.

2.1 Ozonesonde Data at 60 Global Stations

A total of 60 global ozonesonde stations are analyzed to assess the recent stability of the large majority of global network data. All but one station, Hohenpeissenberg (Brewer-Mast type; **Steinbrecht et al., 1998**), currently launch ECC ozonesondes from the two major manufacturers, EnSci and SPC. Ozonesonde stations included in this analysis appear on the map in **Figure 1**, with S20 dropoff stations indicated by the red dots (see Section 2.3 for a brief note on corrected Canadian data; orange dots). Metadata and the data repository accessed for each station are contained in **Table 1**. Of the 60 ozonesonde sites, 37 have had their data homogenized according to ASOPOS/ASOPOS 2.0 standards (Section 1). There are 42,042 ozonesondes analyzed for the 60 stations in our study period of August 2004 to present.

All ozonesonde profile data are first placed into 100 m binned averages. To obtain TCO from the ozonesondes, an identical method to S20 is used: The ozonesonde ozone is integrated up to 10 hPa or balloon burst, whichever is lower in altitude, and the **McPeters and Labow (2012)** ozone climatology is added to that value to obtain TCO. Any ozonesonde not reaching 30 hPa is discarded from the TCO data set.

2.2 Satellite and Ground-Based Ozone Data

Satellite TCO and stratospheric ozone profile data are used as references to evaluate the quality of the past 18 years (since mid-2004) of global ozonesonde network data. Ground-based TCO (Dobson, Brewer, SAOZ) measurements from the World Ozone and Ultraviolet Data Centre (WOUDC) are available at 40 of the 60 stations (**Table 1**). While ground-based TCO comparisons are typically preferred over satellite data, unfortunately, as discussed in S20, a number of the affected dropoff stations (e.g., Costa Rica, San Cristóbal, Ascension, Fiji,

Kelowna, Yarmouth) do not have ground-based measurements available. However, the characteristics of the ozonesonde dropoff and sudden TCO low bias at stations such as Hilo are identified by both satellite and ground-based Dobson and Brewer data (see Figure S4 in S20). Level 2 (L2) satellite TCO and stratospheric ozone overpass data from multiple satellites are available at all 60 stations.

All L2 satellite overpass data are collected from NASA/GSFC's Aura Validation Data Center (AVDC; <https://avdc.gsfc.nasa.gov/pub/data/satellite/>). There are five satellite instruments included for analysis. For TCO, we use Aura OMI (**McPeters et al., 2008; 2015**), the Suomi National Polar-orbiting Partnership Ozone Mapping and Profiler Suite (OMPS; **McPeters et al., 2019**), the Meteorological Operational satellites A/B Global Ozone Monitoring Experiment-2 (MetOp-A/B GOME-2A/2B; **Munro et al., 2016**), and for stratospheric ozone Aura MLS (**Froidevaux et al., 2008; Livesey et al., 2021**). The Aura MLS instrument team recently released the v5 ozone data used here (**Livesey et al., 2022**), which show negligible differences in the stratosphere compared to v4.2 (used in S20; MLS Version 5.0x Level 2 and 3 data quality and description document: **Livesey et al., 2021**).

MetOp-A (GOME-2A) was retired in November 2021 and data are unavailable thereafter. In general, GOME-2A/B measure higher TCO amounts than OMI and OMPS (**Figure S1**), a result consistent with that observed in comparisons to the ozonesonde data in Section 3, and in the analysis of GOME-2A/B compared to ground-based Dobson and Brewer TCO by **Hao et al. (2014)**. OMI has a continuous, nearly 18-year record and is the primary satellite TCO instrument used in our analysis.

The ozonesonde/satellite overpass coincidence criteria are as follows: For satellite TCO comparisons, the L2 data are restricted to within 12 hours and 100 km of the ozonesonde launch. The ± 12 hour coincidence criterion was chosen to ensure that virtually every ozonesonde had a candidate satellite TCO comparison (e.g., to account for days when the station was located between satellite measurement swaths). No filtering for satellite cloud fraction is applied. As discussed in S20, cloud fraction filtering produces no appreciable change to our results. Only one satellite TCO measurement (closest in time and space) from each instrument is matched to each ozonesonde. An addition to this analysis is that satellite/ozonesonde (and ground-based) TCO differences beyond $\pm 20\%$ are discarded as outliers, although this is rare. Just 0.8%, or 246 of all ozonesonde/OMI TCO comparisons exceed $\pm 20\%$. These outliers are mostly confined to mid- to high-latitudes, but no clear pattern emerges to otherwise explain the causes for the cases of poor agreement. For Aura MLS stratospheric ozone, all ozone profiles within 1 day, $\pm 5^\circ$ latitude, and $\pm 8^\circ$ longitude of the ozonesonde are averaged, and the 100 m-averaged ozonesonde data are linearly interpolated to the MLS pressure levels to make comparisons. As with S20, the MLS weighting functions are not applied to the ozonesonde data.

Comparisons among satellite and ground-based TCO data are included in **Figure S1**. These indicate the relative stability of satellite TCO compared to ground-based measurements during our study period, and that the satellite TCO data are a consistent reference suitable for characterizing the ozonesonde network data quality.

The total number of available ozonesonde comparisons are as follows: 30,751 for OMI (Oct. 2004-present), 19,280 for OMPS (Jan. 2012-present), 22,026 for GOME-2A (Jan. 2007-Nov. 2021), 15,317 for GOME-2B (Jan. 2013-present), and 39,703 for Aura MLS (Aug. 2004-present).

2.3 Focus of Analysis: Ozonesonde Network Data Stability and TCO Drop Status

Our primary focus is on expanding the analysis of ozonesonde/satellite TCO and stratospheric ozone comparisons to assess the accuracy and stability of ozonesonde network data over the past two decades. The 14 S20 “dropoff” stations will still be used here as a reference to characterize the effects of the TCO drop, and an analysis of ECC S/Ns is leveraged to investigate potential biases at “unaffected” stations including the 23 stations not appearing in S20 (total of 46 “non-S20” stations). To quantify the magnitude of the TCO drop, we determine the timing, based on EnSci S/N, of a step change in ozonesonde TCO using the Matlab function *ischange*, which locates breakpoints in a time series by finding abrupt changes to the mean values for segments of the dataset. Detailed documentation on *ischange* can be found at <https://uk.mathworks.com/help/matlab/ref/ischange.html>, which is based on work by **Killick et al., (2012)**. The function was applied to the OMI and EnSci ECC TCO percentage differences for the EnSci S/Ns at the 14 S20 stations. The *ischange* function iteratively minimizes cost functions to determine how well segments of the dataset are represented by its mean, and we use this method to identify the single largest change in the mean of the OMI and EnSci ECC TCO comparisons.

Of the 60 global stations used here, 37 have homogenized their time series (see **Table 1**). It should be noted that step changes in TCO of both signs are found in the data of a select few non-homogenized stations (e.g. Scoresbysund and Idabel for EnSci, Legionowo for SPC). The step changes in non-homogenized time series can be significant as shown in previous studies (e.g., **Witte et al., 2017; Sterling et al., 2018; Ancellet et al., 2022**). However, these are often the result of instrumental, station operational, or data processing changes, and are typically removed with homogenization.

Since the publication of S20, the data from two Canadian “dropoff” stations, Kelowna and Yarmouth, have been properly homogenized by applying a transfer function for use of the 1% KI, full buffer SST in the EnSci ozonesonde (**Deshler et al., 2008**). The resulting update to the Canadian data homogenization reduces the pre-2015 EnSci TCO by approximately 4%. The corrected versions of the data are used here, which indicates that Kelowna and Yarmouth are not nearly as affected by the TCO drop as reported in S20, although a small dropoff remains at both stations (Kelowna is shown in **Figure S2**). The Canadian network has since switched to the SPC ozonesonde, mitigating the ~2-3% TCO drop found in the network’s EnSci time series (**Figure S3**). For simplicity, we retain the 14 S20 TCO drop stations in this analysis to describe the effects of the dropoff. As indicated below, data users should refer to **Table 2** to gauge the effects of the TCO drop at EnSci stations in this analysis. Because of the corrected Kelowna and Yarmouth data, corrections to the applied stratospheric pump efficiencies at Costa Rica in 2013-2015, and the addition of 23 more stations including several with newly homogenized data, the results here supersede those presented in S20.

The focus of our analysis is as follows: 1) In light of the TCO dropoff, we assess the overall stability of the global ozonesonde network data and examine the ozonesonde time series from stations grouped into latitudinal bands, commonly used to report ozone trends in the WMO/UNEP Ozone Assessment Reports and related activities (**WMO, 2018; Petropavlovskikh et al., 2019**). 2) We scrutinize the S/Ns of the ECCs to pinpoint step changes in the global network data, and more precisely define which and to what degree stations are affected by the TCO drop.

3 Results

3.1 Ozone-sonde Comparisons with Five Satellite Instruments since 2004

We begin with an analysis of the past ~18 years of ozone-sonde network data compared to satellite measurements to examine the overall stability of the measurements. Since ozone-sonde ozone trends are typically computed for stations within prescribed latitude (ϕ) bands, we examine ozone-sonde/satellite TCO and stratospheric ozone comparisons for various latitudinal regions. In **Figure 2** we present the time series of ECC TCO and stratospheric ozone comparisons with the five satellite instruments for all 60 stations. The top panel of **Figure 2** shows the comparisons with Aura MLS on MLS pressure levels, which gives no indication of any sustained low or high biases in the stratosphere above 50 hPa. The **Figure 2** middle panel shows the time series of 500-point centered, moving averages for TCO comparisons in percent difference. The moving average comparisons with OMI deviate by no more than $\pm 2\%$ over the 18-year record. In general, the ozone-sondes measure lower relative to GOME-2A/B, as is also the case for the ground-based TCO data compared to GOME-2A/B (see **Figure S1**).

The bottom panel of **Figure 2** shows the 25th to 75th percentile, and median comparisons with the four TCO satellite instruments for each year from 2005-2021. The middle and bottom panels of **Figure 2** indicate a slight drop in the ozone-sonde measurements relative to satellite data in 2016-2018. However, for all four satellite instruments and for each year, the interquartile range of the TCO comparisons always encompasses the 0% line. Considering all available data, the means \pm one standard deviation of ozone-sonde TCO comparisons with the four satellite instruments for the 60 global stations are $+0.0 \pm 4.8\%$ ($\mu \pm 1\sigma$; OMI), $-0.8 \pm 4.8\%$ (OMPS), -1.9

$\pm 4.9\%$ (GOME-2A), and $-2.2 \pm 4.8\%$ (GOME-2B). Overall, the global ozonesonde network data are remarkably accurate and stable relative to the satellite data since late 2004.

Figures 3-5 present the same analysis as **Figure 2** for various latitudinal groupings of ozonesonde stations. The ozonesonde measurements at polar stations ($|\phi| \geq 60^\circ$; 17 stations) shown in **Figure 3** are arguably more stable relative to the satellite TCO than the network as a whole in **Figure 2**. Again, the ozonesondes measure lower relative to GOME-2A/B compared to OMI and OMPS. This is a common feature across all latitudes. The midlatitude stations (**Figure 4**; $20^\circ \leq |\phi| < 60^\circ$; 31 stations) display a similar pattern in the time series as the entire global network, which is not surprising since mid-latitudes comprise the densest distribution of stations. A small decrease in the ozonesonde TCO measurements relative to satellites is noted between ~2017-2018. However, the deviation of the OMI comparison moving averages in **Figure 4** never exceeds $\pm 2\%$, and the interquartile range of the comparisons for each year encompasses the 0% line for all four satellite TCO instruments in both **Figures 3 and 4**. We note the apparent annual cycle, which is out of phase for OMI/OMPS and GOME-2A/B, in the ozonesonde/satellite comparisons at the mid-latitude stations in **Figure 4**. This cycle in GOME-2A/B TCO is clearly shown by **Hao et al., (2014; their Figure 13)**, which also indicates that GOME-2A/B measure about 1 to 2% higher than ground-based Dobson and Brewer TCO, and matches our results.

The tropical ozonesonde stations (**Figure 5**; $|\phi| < 20^\circ$; 12 stations) measure within approximately 0 to -2% relative to OMI TCO for the entire period from 2005-2014. After 2014, there is a marked decrease in ozonesonde stratospheric ozone mixing ratio and TCO compared to satellites. The maximum low bias occurs in 2016-2017, when the tropical ozonesondes average 4-6% low relative to the satellite TCO. A notable drop in the stratospheric ozone comparisons with Aura MLS also appears during this period, indicated by the increased blue coloring on the

top panel of **Figure 5**. The overall means and standard deviations of ozonesonde comparisons with the four satellite instruments for the 12 tropical stations are $-2.2 \pm 4.0\%$ (OMI), $-2.9 \pm 3.8\%$ (OMPS), $-2.8 \pm 4.1\%$ (GOME-2A), and $-4.0 \pm 3.9\%$ (GOME-2B). Even prior to the low bias period that begins in 2014, the tropical ozonesondes measure consistently low relative to the satellite TCO. The ozone partial pressure peak at tropical latitudes occurs at approximately 20 hPa, compared to ~ 50 hPa at mid- and high-latitudes. Thus, stratospheric pump efficiency corrections have more impact on the calculation of ozone partial pressure and TCO in the tropics, and any under/overestimation of applied ECC pump efficiencies will have a larger effect in the tropics compared to the extratropics. This is a topic for further investigation by the ASOPOS 2.0 panel.

The low biases in the tropical ozonesonde network improved slightly after 2017, with a relative increase in the ozonesonde measurements of about 2% TCO in the past 3-4 years. However, the TCO drop of several percent relative to satellite measurements from 2014-2017 may affect calculations of ozone trends using tropical ozonesonde data. Data users are advised to proceed with caution when computing tropical TCO and stratospheric ozonesonde trends over the past \sim two decades. While we show that, on average, tropical stations show larger TCO low biases associated with the TCO drop, it is important to note that not all tropical stations are affected by this sudden low bias. More discussion on the dropoff affected stations and magnitudes of the TCO drop are found in Section 3.2.

Figure 6 provides a closer examination of the stratospheric ozonesonde measurement comparisons with the Aura MLS instrument since late 2004. The profile comparisons in percent difference (25th, 50th, and 75th percentiles) are presented for the same groups of stations (**Figure 6a-d**) as in **Figures 2-5**. In general, the ozonesonde network agreement with Aura MLS is

excellent, and lies within $\pm 5\%$ from 50 to 10 hPa. Because a number of factors can decrease the reliability of ozonesonde data above 10 hPa (e.g., the effects of boiling or freezing ozonesonde solutions, decreasing ozonesonde pump efficiencies/increasing pump efficiency uncertainties), we choose to halt ozonesonde integration at 10 hPa prior to adding the **McPeters and Labow (2012)** above-burst climatology when computing the ozonesonde TCO (as in S20). The tropical (**Figure 6d**) stratospheric ozonesonde profiles measure slightly low relative to MLS compared to the other latitude bands, a result likely compounded by the increased low bias from 2014 to 2018 noted in the **Figure 5** top panel. As S20 showed, the dropoff appears to be confined to pressures above ~ 50 hPa, except at Hilo and Costa Rica where there is anomalously low ozone in the troposphere. With these two exceptions, tropospheric ozone data from sondes are reliable for determining ozone trends in the tropics (**Thompson et al., 2021**).

Figures 2-6 show that the TCO dropoff described in S20 has only a minor effect on the overall stability of global ozonesonde network data, and that the data should be considered reliable for trends analysis. However, when considering only tropical stations, the TCO drop will potentially have a detectable effect on ozone trends. The rest of the analysis focuses on expanding the S20 analysis to characterize the effects and timing of the TCO drop found at a subset of stations.

3.2 Status Update to the TCO Dropoff

Figures 2-6 indicate that the effects of the TCO drop described in S20 are most pronounced in the tropical ozonesonde network. As yet, undetermined manufacturing changes to the EnSci ozonesonde are suspected to be a factor in the TCO drop. Because S/N is a better

indicator of a potential manufacturing change than date of ozonesonde launch, the remainder of our analysis focuses on ECC S/Ns to pinpoint the timing of the dropoff.

Figure 7 updates a similar ECC S/N analysis that was presented in S20 (see also **Figure S3**). The bars on **Figure 7** span the 25th to 75th percentiles in percent TCO agreement with OMI for EnSci S/Ns placed in bins of 1000, with the dots representing the median value. Total valid ECC/OMI comparisons are indicated by the numbers along the top and bottom of the figure for each S/N bin of 1000. The EnSci S/Ns from the 14 S20 stations are shown on (a), and the EnSci S/Ns from the remaining “non-S20” stations are shown on (b). Panel (a) in **Figure 7** makes clear the effects of the TCO drop on the ozonesonde comparisons with OMI after S/N 25000. The dropoff is approximately 3 to 5% when considering the 14 stations. There is also a notable drop for S/N ~21-22000s, a “recovery” for 23-24000s, and a sharp drop and persistent low bias beginning with 25000. **Figure 7b** shows that the non-S20 dropoff stations’ median TCO comparisons with OMI have remained within $\pm 2\%$ for all S/Ns through the 35000s. **Figure 7b** also illustrates the importance of ongoing ozonesonde data evaluation, as the most recent data (36000-38000) display a median low bias of up to 2.6%.

This expanded analysis of 60 global stations confirms that only the EnSci ECC displays the characteristics of the ozonesonde TCO drop. **Figure 8** shows an identical analysis to **Figure 7** for all SPC 6A ozonesondes. Note that the similar S/N values to EnSci are a coincidence. The variation in TCO agreement in the SPC 6A S/N bins is larger than that for the 46 non-S20 EnSci stations. This suggests that SPC ECCs are also subject to possible variations in production and thus data quality. However, there are no extended periods of high or low biases similar to those displayed by the S20 dropoff stations in **Figure 7a**. For this reason, we confine the rest of our TCO drop analysis to the EnSci ECCs.

A closer examination of the individual EnSci S/Ns, rather than through binning them into sets of 1000, allows a better estimate of the timing of the step change in ozonesonde TCO agreement with OMI. The location of the step change was determined using the Matlab function *ischange*, which is found at EnSci S/N 25250. We use the 25250 S/N as a reference to divide the ozonesondes into two groups to quantify a single step change in ozonesonde TCO for all EnSci stations. There is a nearly 4% (from +0.42 to -3.5%) TCO drop relative to OMI for the 14 S20 stations after S/N 25250 as shown in **Figure 9a**. Prior to S/N 25250, the standard deviation of the EnSci/OMI comparisons is 4.3%, and after S/N 25250 it is 4.4%. This indicates that the TCO drop is indeed a step change, with no change to the variance in the TCO comparisons with OMI. This potentially means that the uncertainties of the affected EnSci ozonesonde measurements have not increased, but future analyses are still needed to fully characterize these results.

The same analysis technique applied to all the EnSci ozonesondes at the non-S20 stations (**Figure 9b**) indicates that there may also be a detectable TCO drop, albeit just over 1% (mean differences with OMI change from +0.68 to -0.39%), at those stations. Both the S20 and non-S20 station step-changes in the mean values from pre- to post-S/N 25250 are statistically significant based on a 95% confidence interval (see text on **Figures 9a and 9b**). This interval is determined using 10,000 bootstrap resamples of each distribution to generate the confidence bounds around the mean value (**Efron 1979; Efron and Tibshirani 1993**). The 1% TCO drop for non-S20 stations appears to support the hypothesis posed in S20 that a production change in the EnSci ozonesonde is a factor leading to the dropoff, which leads to station-specific preparation procedures, sensing solution type, or other factors mitigating, or amplifying the effects of this production change.

The largest TCO drop for the EnSci ECCs is found relative to OMI. The S20 station TCO drops compared to the other three satellite instruments (**Figure S4**) are smaller in magnitude at less than 3%. The TCO drops for the non-S20 stations are statistically *insignificant* for OMPS and GOME-2A (**Figure S5**). Determining whether there has been a drift in OMI TCO or one of the other three satellites is beyond the scope of this paper, but the smaller ozonesonde TCO drops relative to OMPS, GOME-2A, and GOME-2B, albeit with shorter available time series, are an important consideration.

The pre- and post-S/N 25250 percent change in TCO relative to OMI for each station is shown in **Table 2**, provided that 25 valid OMI comparisons are available for both periods. When considering *all* EnSci ECCs, the pre- to post-S/N 25250 TCO drop relative to OMI is 1.8%.

Time series of comparisons with the five satellite instruments (including GOME-2C) are posted to https://tropo.gsfc.nasa.gov/shadoz/SHADOZ_PubsList.html so that users can examine the ozonesonde data stability relative to satellite measurements for all 60 stations since late 2004.

Table 2 should be used in conjunction with the posted station time series to assess the potential effects of the EnSci TCO drop, and to identify other biases or step changes in the ozonesonde data at specific stations.

The effects of the TCO drop on the ozonesonde stratospheric profiles relative to Aura MLS measurements are shown in **Figure 10**. The S20 stations (**Figure 10a**) show roughly a 3-5% decrease in stratospheric ozone, with the median post-S/N 25250 values being lower than MLS at all pressure levels from 56.23 to 6.81 hPa. The non-S20 stations (**Figure 10b**) show a smaller drop of 1-2% ozone relative to MLS from pre- to post-S/N 25250. Oscillations in the Aura MLS ozone profiles, which have been reduced but still exist in the v5 data (**Livesey et al., 2022**), in the tropical upper troposphere/lower stratosphere make it difficult to exactly quantify

the stratospheric ozone drop at and below the 56.23 hPa level. However, other than the Costa Rica and Hilo stations previously mentioned, we do not find evidence that the TCO drop affects altitudes/pressures below this pressure level or in the troposphere.

3.3 Potential Indicators of the Source of the Dropoff

We explore a possible relationship of the TCO drop with the SST used at each station. Three SSTs are currently in use in the global network: 1% KI, full buffer (SST1.0); 0.5% KI, half buffer (SST0.5); 1.0% KI, one-tenth buffer (SST0.1; “low-buffer”). Tropical/subtropical stations are where the largest and most persistent TCO drops are found. Five of the seven tropical S20 EnSci stations use SST0.1 (Hilo, Costa Rica, San Cristóbal, Fiji, and Samoa) and show a larger post-S/N 25250 dropoff compared to the two SST0.5 stations (Nairobi and Ascension Island; 3.8% average for SST0.1 vs. 2.7% average for SST0.5; Ascension Island is listed at “N/A” in **Table 2** because it did not launch EnSci ECCs prior to S/N 25250). Given this fact and the results of **Figure 9b**, which indicate that non-S20 stations may also show small TCO drops, it is prudent to examine SST0.1 stations outside of tropical/subtropical latitudes.

Figure S6a presents an analysis of the EnSci S/Ns at three stations in the Contiguous U.S. (CONUS): Trinidad Head, Boulder, and Huntsville, that have used SST0.1 since 2005 (Sterling et al., 2018). The three stations show a TCO drop of 1.7% (significant with > 95% confidence) relative to OMI after EnSci S/N 25250, and now average -1.43% TCO relative to OMI. **Figure S6b** shows the Boulder EnSci S/N comparisons with the co-located Dobson TCO, which confirms the OMI results. The Boulder ozonesondes show a sharp 1.8% TCO drop (again, significant with > 95% confidence) relative to the Dobson after S/N 25250. From the results presented above, it appears that all EnSci stations may be subject to some change in ECC

performance related to the TCO drop, with the magnitude of effects possibly dependent on station-specific characteristics such as the SST formula. Although our analysis suggests a potential role for SST type in the dropoff, this must be empirically tested in the laboratory and field before drawing definitive conclusions. In general, SST0.5, which is the ASOPOS-recommended SST for the EnSci ECC, is apparently less affected at global network stations. We point out that several stations using the low-buffer SST0.1 solution are affected by the TCO drop. However, the S20 study effectively ruled out other potential sources of the sudden EnSci low bias including the type of radiosonde paired with the ozonesondes and radiosonde pressure offsets (Steinbrecht et al., 2008; Stauffer et al., 2014; Inai et al., 2015).

A large dataset of lab-measured EnSci pump efficiency corrections by **Nakano and Morofuji (2022)** shows that changing stratospheric pump efficiencies are a potential contributor to the TCO drop. Their analysis indicates that larger pump efficiency corrections above 50 hPa are necessary for EnSci ECCs beginning with S/N ~25000 (see their Figure 15). Raw ozonesonde ECC cell currents are processed using an average pump efficiency that is assumed to not vary significantly based on ECC production and S/N. However, application of the larger **Nakano and Morofuji (2022)** pump efficiency corrections after S/N 25000 will increase EnSci ECC stratospheric ozone and TCO. Also note on their Figure 15 the *lower* pump efficiency corrections for S/N 24000s, which corresponds to the high-biased ozonesonde TCO for S20 stations on **Figure 7a**.

The ASOPOS Task Team will quantify the effects that the **Nakano and Morofuji (2022)** pump corrections have on EnSci ozone time series, and determine if the TCO drop is mitigated with the application of their lab-measured pump efficiencies. A change to the EnSci stratospheric pump efficiencies would explain why it appears that, on average, all EnSci stations may show at

least a small TCO drop coincident with S/N 25250. Furthermore, because the tropical stratospheric ozone peak is found at higher altitudes/lower pressures compared to mid- and high-latitude stations, larger than expected EnSci stratospheric pump efficiency corrections would disproportionally affect TCO at tropical sites, potentially explaining the clustering of S20 stations in the tropics.

A discussion on our communications with the EnSci manufacturer is found in the Supplementary Material.

4 Summary and Discussion

We have presented the first examination of data quality from the 60-station global ozonesonde network using the ASOPOS 2.0 guidelines that recommend comparison of sonde TCO and stratospheric ozone profiles with consistently calibrated and updated satellite data. We evaluated ozonesonde network data since late 2004 by comparing satellite TCO and stratospheric ozone measurements with ~40,000 ECC profiles from the 60 stations. This investigation extends our 37-station S20 study and adds measurements from 2020-2022. The expanded analysis reveals that overall, the ozonesonde measurements are stable and accurate relative to satellite TCO and stratospheric measurements over the past 18 years. Average ozonesonde TCO comparisons with Aura OMI remain within $\pm 2\%$ for each year from 2005 to 2021. Ozonesonde TCO stability is slightly better relative to OMPS and GOME-2A/B, over shorter periods. Stratospheric ozone measurements from ozonesondes also agree within $\pm 5\%$ of Aura MLS data for all stations and pressure levels from 50 to 10 hPa. However, the TCO dropoff affects about half of tropical ($\pm 20^\circ$ latitude) ECC stations, with an overall average 4-6% TCO low bias relative to four satellite instruments in 2016-2017 at tropical latitudes. A new dataset of lab-measured

EnSci stratospheric pump efficiencies offers a promising path toward investigating the role of the ECC pump for TCO drop-affected station data (**Nakano and Morofuji, 2022**).

The results described above reinforce the importance of following the ASOPOS 2.0 guidelines for continuous evaluation of ECC sonde data quality with satellite observations as well as with co-located ground-based instruments: Dobson, Brewer, SAOZ, Fourier Transform InfraRed (FTIR), Microwave (MW), lidar. TCO data from OMI, OMPS, GOME-2A/B, and stratospheric ozone profile data from Aura MLS are available as L2 overpass files for all 60 stations used in this analysis, and dozens more (websites in Acknowledgments and Data Availability Statement). The availability of these files eliminates cumbersome downloading of full satellite ozone datasets. With such streamlining, the sonde community has an “early warning system” for unexpected changes to a station’s instrumentation or preparation procedures. The satellite and ground-based instrument comparisons also serve as a guide for homogenizing data from ozonesonde time series. Comparisons among ozonesonde and satellite data since the beginning of the Aura OMI record in late 2004 for all 60 stations used in this study have been posted to https://tropo.gsfc.nasa.gov/shadoz/SHADOZ_PubsList.html.

Finally, our assessment has shown that the global ozonesonde network data are of exceptionally high quality overall. This is especially true given the success of ozonesonde data homogenization that has been applied to dozens of stations, reducing or eliminating step changes and biases in the non-homogenized time series. The metric of 5% uncertainty in the ozonesonde measurement, requested by the satellite and trends communities is nearly achieved. As data from additional stations are homogenized, users will see greater uniformity in ozone profile quality throughout the global network data.

Acknowledgments

The data analysis that contributed to this paper is part of an ongoing effort by the ASOPOS 2.0 Panel and ozonesonde colleagues to quantify global ozonesonde network data quality and to solve the TCO dropoff. The authors express appreciation to the Network for the Detection of Atmospheric Composition Change (NDACC) Ozonesonde Working Group and Steering Committee. The ozonesonde data collected and presented here represent the combined effort of hundreds of ozonesonde community members around the globe, for which we are grateful. We are also grateful for the open communication from EnSci to help solve the source of the ozonesonde TCO drop. Funding for this work was graciously provided through support of SHADOZ and NDACC by the NASA Upper Atmosphere Research Program and Upper Atmospheric Composition Observations Program (UARP and UACO; Dr. Kenneth Jucks program manager) to NASA/GSFC (R. M. Stauffer, PI). Special thanks to Universidad San Francisco de Quito (USFQ) and to Dr. María Cazorla, PI, for providing and making public the ozonesonde data from Ecuador (**Cazorla et al., 2021**).

Open Research

The following URLs were accessed for ozonesonde data, and specific stations corresponding to the various archives can be found in Table 1 of this manuscript: National Oceanic and Atmospheric Administration (NOAA/GML, 2022): <ftp://ftp.gml.noaa.gov/data/ozwv/Ozonesonde/>; Harmonization and Evaluation of Ground Based Instruments for Free Tropospheric Ozone Measurements (HEGIFTOM; RMI, 2022): <http://hegiftom.meteo.be>; Universidad San Francisco de Quito (USFQ, 2022): <https://observaciones-iiia.usfq.edu.ec/>; Network for the Detection of Atmospheric Composition

Change (NDACC, 2022): <https://www-air.larc.nasa.gov/missions/ndacc/data.html>; World Ozone and Ultraviolet Data Centre (WOUDC, 2022): <https://woudc.org/data/explore.php?lang=en> (<http://dx.doi.org/10.14287/100000008>; WOUDC, 2022a); SHADOZ: <https://tropo.gsfc.nasa.gov/shadoz/Archive.html> (<https://doi.org/10.57721/SHADOZ-V06>; NASA/GSFC, 2019); Tropospheric Ozone Pollution Project (TOPP; Rice, 2022): <http://www.ruf.rice.edu/~ozone/>. Ground-based TCO data were downloaded from WOUDC: (<http://dx.doi.org/10.14287/100000004>; WOUDC, 2022b). Aura MLS v5 L2 ozone profile overpass data were downloaded at <https://avdc.gsfc.nasa.gov/pub/data/satellite/Aura/MLS/V05/L2GPOVP/O3/> (NASA/GSFC, 2022a). OMI, OMPS, GOME-2A, and GOME-2B L2 TCO overpass data were downloaded at <https://avdc.gsfc.nasa.gov/pub/data/satellite/Aura/OMI/V03/L2OVP/OMTO3/> (NASA/GSFC, 2022b), https://avdc.gsfc.nasa.gov/pub/data/satellite/Suomi_NPP/L2OVP/NMTO3-L2/ (NASA/GSFC, 2022c), <https://avdc.gsfc.nasa.gov/pub/data/satellite/MetOp/GOME2/V03/L2OVP/GOME2A/> (NASA/GSFC, 2022d), and <https://avdc.gsfc.nasa.gov/pub/data/satellite/MetOp/GOME2/V03/L2OVP/GOME2B/> (NASA/GSFC, 2022e). Time series of the comparisons of satellite and ozonesonde data for all 60 stations used in this study can be found at https://tropo.gsfc.nasa.gov/shadoz/SHADOZ_PubsList.html (NASA/GSFC, 2022f). All analyses were performed using the MATLAB 2017b software package (<https://uk.mathworks.com/help/matlab/release-notes-R2017b.html>; MATLAB, 2017).

References

- Ancellet, G., Godin-Beekmann, S., Smit, H. G. J., Stauffer, R. M., Van Malderen, R., Bodichon, R., & Pazmiño, A. (2022). Homogenization of the Observatoire de Haute Provence ECC ozonesonde data record: comparison with lidar and satellite observations, *Atmospheric Measurement Techniques*, 15, 3105–3120, <https://doi.org/10.5194/amt-2022-7>.
- Boyd, I., Bodeker, G., Connor, B., Swart, D., & Brinksma, E. (1998). An assessment of ECC ozone sondes operated using 1% and 0.5% KI cathode solutions at Lauder, New Zealand. *Geophysical Research Letters*, 25, 2409–2412, doi:10.1029/98GL01814.
- Cazorla, M., Parra, R., Herrera, E., da Silva, F., R. (2021). Characterizing ozone throughout the atmospheric column over the tropical Andes from in situ and remote sensing observations. *Elementa: Science of the Anthropocene* 21, 9 (1): 00019. <https://doi.org/10.1525/elementa.2021.00019>.
- Cooper, O. R., Parrish, D. D., Stohl, A., Trainer, M., Nédélec, P., Thouret, V., et al. (2010). Increasing springtime ozone mixing ratios in the free troposphere over western North America. *Nature*, 463, 344–348. <https://doi.org/10.1038/nature08708>.
- Davies, J., McElroy, C. T., Tarasick, D. W., & Wardle, D. I. (2003). Ozone capture efficiency in ECC Ozonesondes; measurements made in the laboratory and during Balloon Flights. EGS-AGU-EUG Joint Assembly, Abstracts from the meeting held in Nice, France, 6–11 April 2003. Abstract id: 13703.
- Deshler, T., Mercer, J., Smit, H. G. J., Stuebi, R., Levrat, G., Johnson, B. J., et al. (2008). Atmospheric comparison of electrochemical cell ozonesondes from different manufacturers, and with different cathode solution strengths: The Balloon Experiment on Standards for Ozonesondes. *Journal of Geophysical Research*, 113, D04307, doi:10.1029/2007JD008975.

Deshler, T., Stuebi, R., Schmidlin, F. J., Mercer, J. L., Smit H. G. J., Johnson, B. J., et al. (2017).

Methods to homogenize electrochemical concentration cell (ECC) ozonesonde measurements across changes in sensing solution concentration or ozonesonde manufacturer. *Atmospheric Measurement Techniques*, 10, 2021–2043, doi:10.5194/amt-10-2021-2017.

Efron, B. (1979). Bootstrap Methods: Another Look at the Jackknife." *Ann. Statist.* 7 (1) 1 - 26, January, 1979. <https://doi.org/10.1214/aos/1176344552>.

Efron, B. & Tibshirani, R.J. (1993). *An Introduction to the bootstrap*. Chapman and Hall, Boca Raton.

Froidevaux, L., Jiang, Y. B., Lambert, A., Livesey, N. J., Read, W. G., Waters, J. W., et al. (2008). Validation of Aura Microwave Limb Sounder stratospheric ozone measurements. *Journal of Geophysical Research*, 113, D15S20, doi:10.1029/2007JD008771.

Hao, N., Koukouli, M. E., Inness, A., Valks, P., Loyola, D. G., Zimmer, W., Balis, D. S., Zyrichidou, I., Van Roozendaal, M., Lerot, C., and Spurr, R. J. D. (2014). GOME-2 total ozone columns from MetOp-A/MetOp-B and assimilation in the MACC system, *Atmos. Meas. Tech.*, 7, 2937–2951, <https://doi.org/10.5194/amt-7-2937-2014>.

Hassler, B., Kremser, S., Bodeker, G. E., Lewis, J., Nesbit, K., Davis, S. M., Chipperfield, M. P., Dhomse, S. S., and Dameris, M. (2018). An updated version of a gap-free monthly mean zonal mean ozone database, *Earth Syst. Sci. Data*, 10, 1473-1490, <https://doi.org/10.5194/essd-10-1473-2018>.

Hubert, D., Lambert, J.-C., Verhoelst, T., Granville, J., Keppens, A., Baray, J.-L., Bourassa, A. E., Cortesi, U., Degenstein, D. A., Froidevaux, L., Godin-Beekmann, S., Hoppel, K. W., Johnson, B. J., Kyrölä, E., Leblanc, T., Lichtenberg, G., Marchand, M., McElroy, C. T., Murtagh, D., Nakane, H., Portafaix, T., Querel, R., Russell III, J. M., Salvador, J., Smit, H.

G. J., Stebel, K., Steinbrecht, W., Strawbridge, K. B., Stübi, R., Swart, D. P. J., Taha, G., Tarasick, D. W., Thompson, A. M., Urban, J., van Gijssels, J. A. E., Van Malderen, R., von der Gathen, P., Walker, K. A., Wolfram, E., & Zawodny, J. M. (2016). Ground-based assessment of the bias and long-term stability of 14 limb and occultation ozone profile data records.

Atmospheric Measurement Techniques, 9, 2497–2534. <https://doi.org/10.5194/amt-9-2497-2016>.

Inai, Y., Shiotani, M., Fujiwara, M., Hasebe, F., & Vömel, H. (2015). Altitude misestimation caused by the Vaisala RS80 pressure bias and its impact on meteorological profiles.

Atmospheric Measurement Techniques, 8, 4043–4054, <https://doi.org/10.5194/amt-8-4043-2015>.

Johnson, B. J., Oltmans, S. J., Vömel, H., Smit, H. G. J., Deshler, T., & Kroeger, C. (2002). ECC ozonesonde pump efficiency measurements and tests on the sensitivity to ozone of buffered and unbuffered ECC sensor cathode solutions. *Journal of Geophysical Research*, 107, D19. <https://doi.org/10.1029/2001JD000557>.

Killick R., P. Fearnhead, and I.A. Eckley (2012). Optimal detection of changepoints with a linear computational cost. *Journal of the American Statistical Association*. 107, 500, 1590-1598.

Komhyr, W. D. (1969). Electrochemical concentration cells for gas analysis. *Annales Geophysicae*, 25, 203–210.

Komhyr, W. D., & Harris, T. B. (1971). Development of an ECC-Ozonesonde. *NOAA Technical Report*. ERL 200-APCL 18. Boulder, CO: U.S. G.P.O.

Komhyr, W. D. (1986). Operations handbook-Ozone measurements to 40-km altitude with model 4A electrochemical concentration cell (ECC) ozonesondes (used with 1680 MHz radiosondes). *NOAA Technical Memo*. ERL ARL-149, Boulder, CO: Air Resources Lab.

Komhyr, W. D., Barnes, R. A., Brothers, G. B., Lathrop, J. A., & Opperman, D. P. (1995).

Electrochemical concentration cell ozonesonde performance evaluation during STOIC 1989.

Journal of Geophysical Research, 100(D5), 9231–9244. <https://doi.org/10.1029/94JD02175>.

Liu, G., J.J. Liu, D.W. Tarasick, V.E. Fioletov, J.J. Jin, O. Moeni, X. Liu, C.E. Sioris and M.

Osman (2013a), A global tropospheric ozone climatology from trajectory-mapped ozone soundings, *Atmos. Chem. Phys.* 13, 10659–10675, <https://doi.org/10.5194/acp-13-10659-2013>.

Liu, J., D.W. Tarasick, V.E. Fioletov, C. McLinden T. Zhao, S. Gong, C. Sioris, J. Jin, G. Liu, and O. Moeini (2013b), A Global Ozone Climatology from Ozone Soundings via Trajectory Mapping: A Stratospheric Perspective, *Atmos. Chem. Phys.*, 13, 11441–11464, <https://doi.org/10.5194/acp-13-11441-2013>.

Livesey, N. J., Read, W. G., Froidevaux, L., Lambert, A., Santee, M. L., Schwartz, M. J., et al. (2021). Investigation and amelioration of long-term instrumental drifts in water vapor and nitrous oxide measurements from the Aura Microwave Limb Sounder (MLS) and their implications for studies of variability and trends. *Atmospheric Chemistry and Physics*, 21, 15409–15430, <https://doi.org/10.5194/acp-21-15409-2021>.

Livesey, N. J., Read, W. G., Wagner, P. A., Froidevaux, L., Santee, M. L., Schwartz, M. J., et al. (2022). Version 5.0x Level 2 and 3 data quality and description document, JPL D-105336 Rev. B. [Available at https://mls.jpl.nasa.gov/data/v5-0_data_quality_document.pdf].

Logan, J. A., Megretskaia, I. A., Miller, A. J., Tiao, G. C., Choi, D., Zhang, L., et al. (1999).

Trends in the vertical distribution of ozone: A comparison of two analyses of ozonesonde data. *Journal of Geophysical Research*, 104, 26373–26400.

Logan, J. A., Jones, D. B. A., Megretskaya, I. A., Oltmans, S. J., Johnson, B. J., Vömel, H.,

Randel, W. J., Kimani, W., and Schmidlin, F. J. (2003). Quasibiennial oscillation in tropical ozone as revealed by ozonesonde and satellite data, *J. Geophys. Res.*, 108, 4244, D8.

doi:10.1029/2002JD002170.

MATLAB. (2017). MATLAB version 9.3.0.713579 (R2017b) [Software]. The Mathworks, Inc.

<https://uk.mathworks.com/help/matlab/release-notes-R2017b.html>.

McPeters, R., Kroon, M., Labow, G., Brinksma, E., Balis, D., Petropavlovskikh, I., et al. (2008).

Validation of the Aura Ozone Monitoring Instrument total column ozone product. *Journal of Geophysical Research*, 113, D15S14, doi:10.1029/2007JD008802.

McPeters, R. D. & Labow, G. J. (2012). Climatology 2011: An MLS and sonde derived ozone

climatology for satellite retrieval algorithms. *Journal of Geophysical Research*, 117, D10303,

doi:10.1029/2011JD017006.

McPeters, R. D., Frith, S., & Labow, G. J. (2015). OMI total column ozone: extending the long-

term data record. *Atmospheric Measurement Techniques*, 8, 4845–4850,

<https://doi.org/10.5194/amt-8-4845-2015>.

McPeters, R., Frith, S., Kramarova, N., Ziemke, J., & Labow, G. (2019). Trend quality ozone

from NPP OMPS: the version 2 processing. *Atmospheric Measurement Techniques*, 12, 977–

985, <https://doi.org/10.5194/amt-12-977-2019>.

Moeini, O., Tarasick, D. W., McElroy, C. T., Liu, J., Osman, M. K., Thompson, A. M., et al.

(2020). Estimating boreal fire-generated ozone over North America using ozonesonde profiles and a differential back trajectory technique. *Atmospheric Environment: X*, 7,

100078. <https://doi.org/10.1016/j.aeaoa.2020.100078>.

Munro, R., Lang, R., Klaes, D., Poli, G., Retscher, C., Lindstrot, R. (2016). The GOME-2 instrument on the Metop series of satellites: instrument design, calibration, and level 1 data processing – an overview, *Atmospheric Measurement Techniques*, 9, 1279–1301, doi:10.5194/amt-9-1279-2016.

Nakano, T. & Morofuji, T. (2022). Development of an automated pump efficiency measuring system for ozonesonde utilizing the airbag type flowmeter, *EGUsphere* [preprint], <https://doi.org/10.5194/egusphere-2022-565>.

NASA/GSFC. (2019). Southern Hemisphere Additional Ozonesondes version 6 ozonesonde profile data [Dataset]. National Aeronautics and Space Administration Goddard Space Flight Center (NASA/GSFC). <https://doi.org/10.57721/SHADOZ-V06>.

NASA/GSFC. (2022a). Aura MLS v5 L2 ozone profile overpass data [Dataset]. National Aeronautics and Space Administration Goddard Space Flight Center (NASA/GSFC). <https://avdc.gsfc.nasa.gov/pub/data/satellite/Aura/MLS/V05/L2GPOVP/O3/>.

NASA/GSFC. (2022b). OMI L2 total column ozone overpass data [Dataset]. National Aeronautics and Space Administration Goddard Space Flight Center (NASA/GSFC). <https://avdc.gsfc.nasa.gov/pub/data/satellite/Aura/OMI/V03/L2OVP/OMTO3/>.

NASA/GSFC. (2022c). OMPS L2 total column ozone overpass data [Dataset]. National Aeronautics and Space Administration Goddard Space Flight Center (NASA/GSFC). https://avdc.gsfc.nasa.gov/pub/data/satellite/Suomi_NPP/L2OVP/NMTO3-L2/.

NASA/GSFC. (2022d). GOME-2A L2 total column ozone overpass data [Dataset]. National Aeronautics and Space Administration Goddard Space Flight Center (NASA/GSFC). <https://avdc.gsfc.nasa.gov/pub/data/satellite/MetOp/GOME2/V03/L2OVP/GOME2A/>.

- NASA/GSFC. (2022e). GOME-2B L2 total column ozone overpass data [Dataset]. National Aeronautics and Space Administration Goddard Space Flight Center (NASA/GSFC). <https://avdc.gsfc.nasa.gov/pub/data/satellite/MetOp/GOME2/V03/L2OVP/GOME2B/>.
- NASA/GSFC. (2022f). Ozonesonde and satellite comparison time series [Figures]. National Aeronautics and Space Administration Goddard Space Flight Center (NASA/GSFC). https://tropo.gsfc.nasa.gov/shadoz/SHADOZ_PubsList.html.
- NDACC. (2022). Network for the Detection of Atmospheric Composition Change ozonesonde profile data [Dataset]. Network for the Detection of Atmospheric Composition Change (NDACC). <https://www-air.larc.nasa.gov/missions/ndacc/data.html>.
- Newton, R., Vaughan, G., Ricketts, H. M. A., Pan, L. L., Weinheimer, A. J., & Chemel, C. (2016). Ozonesonde profiles from the West Pacific Warm Pool: Measurements and validation. *Atmospheric Chemistry and Physics*, 16, 619–634. <https://doi.org/10.5194/acp-16-619-2016>.
- NOAA/GML. (2022). Global Monitoring Laboratory ozone/water vapor group ozonesonde profile data [Dataset]. National Oceanic and Atmospheric Administration Global Monitoring Laboratory (NOAA/GML). <ftp://ftp.gml.noaa.gov/data/ozwv/Ozonesonde/>.
- Petropavlovskikh, I., Godin-Beekmann, S., Hubert, D., Damadeo, R., Hassler, B., & Sofieva, V. (2019). SPARC/IO3C/GAW Report on Long-term Ozone Trends and Uncertainties in the Stratosphere. SPARC Report No. 9, GAW Report No. 241, WCRP Report 17/2018. [Available at https://elib.dlr.de/126666/1/LOTUS_Report_full_noSupplement.pdf].
- Proffitt, M. H., & McLaughlin, R. J. (1983). Fast response dual-beam UV-absorption photometer suitable for use on stratospheric balloons. *Review of Scientific Instruments*, 54, 1719–1728.

Reid, S. J., Vaughan, G., Marsh, A. R. W., & Smit, H. G. J. (1996). Accuracy of ozonesonde measurements in the troposphere. *Journal of Atmospheric Chemistry*, 25, 215–226, <https://doi.org/10.1007/BF00053792>.

Rice University. (2022). Tropospheric Ozone Pollution Project ozonesonde profile data [Dataset]. Rice University. <http://www.ruf.rice.edu/~ozone/>.

RMI. (2022). Harmonization and Evaluation of Ground Based Instruments for Free Tropospheric Ozone Measurements [Dataset]. Royal Meteorological Institute of Belgium (RMI). <http://hegiftom.meteo.be>.

Smit, H. G. J., & Kley, D. (1998). JOSIE: The 1996 WMO International intercomparison of ozonesondes under quasi flight conditions in the environmental simulation chamber at Jülich. Geneva: World Meteorological Organization. WMO Global Atmosphere Watch Report No. 130, WMO TD No. 926.

Smit, H. G. J., & Straeter, W. (2004). JOSIE-2000, Jülich Ozone Sonde Intercomparison Experiment 2000, The 2000 WMO international intercomparison of operating procedures for ECC-ozonesondes at the environmental simulation facility at Jülich. WMO Global Atmosphere Watch report series, No. 158 (Technical Document No. 1225). Geneva: World Meteorological Organization.

Smit, H. G. J., Straeter, W., Johnson, B. J., Oltmans, S. J., Davies, J., Tarasick, D. W., et al. (2007). Assessment of the performance of ECC-ozonesondes under quasi-flight conditions in the environmental simulation chamber: Insights from the Jülich Ozone Sonde Intercomparison Experiment (JOSIE). *Journal of Geophysical Research*, 112, D19306, doi:10.1029/2006JD007308.

Smit, H. G. J. & the Panel for the Assessment of Standard Operating Procedures for Ozonesondes (ASOPOS) (2012). Guidelines for homogenization of ozonesonde data, SI2N/O3S-DQA activity as part of “Past changes in the vertical distribution of ozone assessment”. [Available at http://www-das.uwyo.edu/%7Edeshler/NDACC_O3Sondes/O3s_DQA/O3S-DQA-Guidelines%20Homogenization-V2-19November2012.pdf].

Smit, H. G. J. & the Panel for the Assessment of Standard Operating Procedures for Ozonesondes (ASOPOS) (2014). Quality assurance and quality control for ozonesonde measurements in GAW. World Meteorological Organization, GAW Report 201. [Available at https://library.wmo.int/doc_num.php?explnum_id=7167].

Smit, H. G. J., Thompson, A. M., & the Panel for the Assessment of Standard Operating Procedures for Ozonesondes, v2.0 (ASOPOS 2.0) (2021). Ozonesonde Measurement Principles and Best Operational Practices. World Meteorological Organization, GAW Report 268. [Available at https://library.wmo.int/doc_num.php?explnum_id=10884].

Stauffer, R. M., Morris, G. A., Thompson, A. M., Joseph, E., Coetzee, G. J. R., & Nalli, N. R. (2014). Propagation of radiosonde pressure sensor errors to ozonesonde measurements. *Atmospheric Measurement Techniques*, 7, 65–79, doi:10.5194/amt-7-65-2014.

Stauffer, R. M., Thompson, A. M., & Witte, J. C. (2018). Characterizing global ozonesonde profile variability from surface to the UT/LS with a clustering technique and MERRA-2 reanalysis. *Journal of Geophysical Research: Atmospheres*, 123, 6213–6229. <https://doi.org/10.1029/2018JD028465>.

Stauffer, R. M., Thompson, A. M., Oman, L. D., & Strahan, S. E. (2019). The effects of a 1998 observing system change on MERRA-2-based ozone profile simulations. *Journal of*

Geophysical Research: Atmospheres, 124, 7429– 7441.

<https://doi.org/10.1029/2019JD030257>.

Stauffer, R. M., Thompson, A. M., Kollonige, D. E., Witte, J. C., Tarasick, D. W., Davies, J., et al. (2020). A post- 2013 dropoff in total ozone at a third of global ozonesonde stations: Electrochemical concentration cell instrument artifacts? *Geophysical Research Letters*, 47, e2019GL086791. <https://doi.org/10.1029/2019GL086791>.

Steinbrecht, W., Schwarz, R., & Claude, H. (1998). New pump correction for the Brewer-Mast ozone sonde: Determination from experiment and instrument intercomparisons. *Journal of Atmospheric and Oceanic Technology*, 15, 144–156. [https://doi.org/10.1175/1520-0426\(1998\)015<0144:NPCFTB>2.0.CO](https://doi.org/10.1175/1520-0426(1998)015<0144:NPCFTB>2.0.CO)

Steinbrecht, W., Claude, H., Schöenborn, F., Leiterer, U., Dier, H., & Lanzinger, E. (2008). Pressure and temperature differences between Vaisala RS80 and RS92 radiosonde systems. *Journal of Atmospheric and Oceanic Technology*, 25, 909-927, doi:10.1175/2007JTECHA999.1.

Sterling, C. W., Johnson, B. J., Oltmans, S. J., Smit, H. G. J., Jordan, A. F., Cullis, P. D., et al. (2018). Homogenizing and estimating the uncertainty in NOAA's long term vertical ozone profile records measured with the electrochemical concentration cell ozonesonde. *Atmospheric Measurement Techniques*, 11, 3661-3687, <https://doi.org/10.5194/amt-2017-397>.

Tarasick, D. W., Davies, J., Smit, H. G. J., & Oltmans, S. J. (2016). A re-evaluated Canadian ozonesonde record: Measurements of the vertical distribution of ozone over Canada from 1966 to 2013. *Atmospheric Measurement Techniques*, 9, 195–214, doi:10.5194/amt-9-195-2016.

Tarasick, D. W., Galbally, I., Cooper, O. R., Schultz, M. G., Ancellet, G., LeBlanc, T., et al.

(2019). TOAR-observations: Tropospheric ozone from 1877 to 2016, observed levels, trends and uncertainties. *Elementa: Science of the Anthropocene*, 7(1), 39.

<http://doi.org/10.1525/elementa.376>.

Tarasick, D. W., Smit, H. G. J., Thompson, A. M., Morris, G. A., Witte, J. C., Davies, J., et al.

(2021). Improving ECC ozonesonde data quality: Assessment of current methods and outstanding issues. *Earth and Space Science*, 8, e2019EA000914.

<https://doi.org/10.1029/2019EA000914>.

Thompson, A. M., Witte, J. C., Sterling, C., Jordan, A., Johnson, B. J., Oltmans, S. J., et al.

(2017). First reprocessing of Southern Hemisphere Additional Ozonesondes (SHADOZ) profiles (1998-2016). 2. Comparisons with satellites and ground-based instruments. *Journal of Geophysical Research: Atmospheres*, 122, 13000-13025,

<https://doi.org/10.1002/2017JD27406>.

Thompson, A. M., Smit, H. G. J., Witte, J. C., Stauffer, R. M., Johnson, B. J., Morris, G. A., et

al. (2019). Ozonesonde quality assurance: The JOSIE-SHADOZ (2017) Experience. *Bulletin of the American Meteorological Society*, 100 (1), 155-171, <https://doi.org/10.1175/BAMS-D-17-0311.1>.

Thompson, A. M., Stauffer, R. M., Wargan, K., Witte, J. C., Kollonige, D. E., & Ziemke, J. R.

(2021). Regional and seasonal trends in tropical ozone from SHADOZ profiles: Reference for models and satellite products. *Journal of Geophysical Research: Atmospheres*, 126,

e2021JD034691. <https://doi.org/10.1029/2021JD034691>.

Thornton, D. C., and Niaz, N. (1982), Sources of background current in the ECC ozonesonde: Implications for total ozone measurements, *Journal of Geophysical Research*, 87 (C11), 8943– 8950, doi:10.1029/JC087iC11p08943.

Tilmes, S., Lamarque, J.-F., Emmons, L. K., Conley, A., Schultz, M. G., Saunio, et al. (2012). Technical Note: Ozonesonde climatology between 1995 and 2011: description, evaluation and applications. *Atmospheric Chemistry and Physics*, 12, 7475–7497, <https://doi.org/10.5194/acp-12-7475-2012>.

USFQ. (2022). Universidad San Francisco de Quito ozonesonde profile data [Dataset].

Universidad San Francisco de Quito (USFQ). <https://observaciones-ia.usfq.edu.ec/>.

Van Malderen, R., Allaart, M. A. F., De Backer, H., Smit, H. G. J., & De Muer, D. (2016). On instrumental errors and related correction strategies of ozonesondes: Possible effect on calculated ozone trends for the nearby sites Uccle and De Bilt. *Atmospheric Measurement Techniques*, 9, 3793–3816. <https://doi.org/10.5194/amt-9-3793-2016>.

Vömel, H., & Diaz, K. (2010). Ozone sonde cell current measurements and implications for observations of near-zero ozone concentrations in the tropical upper troposphere. *Atmospheric Measurements Techniques*, 3, 495–505. <https://doi.org/10.5194/amt-3-495-2010>.

Vömel, H., Smit, H. G. J., Tarasick, D., Johnson, B., Oltmans, S. J., Selkirk, H., et al. (2020). A new method to correct the ECC ozone sonde time response and its implications for “background current” and pump efficiency. *Atmospheric Measurements Techniques*, 13, 5667–5680.

Witte, J. C., Schoeberl, M. R., Douglass, A. R., & Thompson, A. M. (2008). The Quasi-biennial Oscillation and annual variations in tropical ozone from SHADOZ and HALOE.

Atmospheric Chemistry and Physics, 8, 3929–3936. <https://doi.org/10.5194/acp-8-3929-2008>.

Witte, J. C., Thompson, A. M., Smit, H. G. J., Fujiwara, M., Posny, F., Coetzee, G. J. R., et al. (2017). First reprocessing of Southern Hemisphere ADditional Ozone-sondes (SHADOZ) profile records (1998–2015): 1. Methodology and evaluation. *Journal of Geophysical Research: Atmospheres*, 122, 6611–6636. <https://doi.org/10.1002/2016JD026403>.

Witte, J. C., Thompson, A. M., Smit, H. G. J., Vömel, H., Posny, F., & Stübi, R. (2018). First reprocessing of Southern Hemisphere ADditional OZonesondes profile records: 3. Uncertainty in ozone profile and total column. *Journal of Geophysical Research: Atmospheres*, 123, 3243–3268. <https://doi.org/10.1002/2017JD027791>.

Witte, J. C., Thompson, A. M., Schmidlin, F. J., Northam, E. T., Wolff, K. R., and Brothers, G. B. (2019). The NASA Wallops Flight Facility digital ozonesonde record: Reprocessing, uncertainties, and dual launches. *Journal of Geophysical Research: Atmospheres*, 124, 3565–3582. <https://doi.org/10.1029/2018JD030098>.

WMO (World Meteorological Organization), Scientific Assessment of Ozone Depletion. (2018). Global Ozone Research and Monitoring Project-Report No. 58. Geneva, Switzerland, p. 588.

WOUDC. (2022a). OzoneSonde [Dataset]. World Ozone and Ultraviolet Data Centre (WOUDC). <http://dx.doi.org/10.14287/10000008>.

WOUDC. (2022b). Total Ozone - Daily Observations [Dataset]. World Ozone and Ultraviolet Data Centre (WOUDC). <http://dx.doi.org/10.14287/10000004>.

Table 1. Metadata for the 60 global ozonesonde stations used in this study including latitude/longitude, number of profiles from August 2004-present, data source, whether the station has co-located ground-based TCO data available in the WOUDC archive, and whether the station's ozonesonde data used here have been homogenized (see text for explanation of the homogenization process). The single asterisks and bold columns indicate the 14 S20 dropoff stations used here as a reference. URLs for the respective ozonesonde data archives are given at the bottom of the table.

Station	Lat (°)	Lon (°)	# Profiles	Dates	Source	Ground-Based?	Homogenized?
Alert*	82.49	-62.34	705	2004-2020	HEGIFTOM	Y	Y
Eureka*	79.98	-85.94	1064	2004-2021	HEGIFTOM	Y	Y
Ny-Ålesund	78.92	11.93	1245	2004-2020	NDACC	Y	N
Thule	76.53	-68.74	118	2004-2016	NDACC	N	N
Resolute	74.7	-94.96	622	2004-2021	HEGIFTOM	Y	Y
Summit	72.34	-38.29	635	2004-2017	NOAA	N	Y
Scoresbysund	70.48	-21.97	849	2004-2021	NDACC	Y	N
Sodankyla	67.37	26.65	670	2004-2019	NDACC	Y	N
Lerwick	60.13	-1.18	621	2004-2016	WOUDC	Y	N
Churchill*	58.74	-94.07	510	2004-2021	HEGIFTOM	Y	Y
Edmonton*	53.54	-114.1	766	2004-2021	HEGIFTOM	Y	Y
Goose Bay	53.31	-60.36	761	2004-2021	HEGIFTOM	Y	Y
Legionowo	52.4	20.97	974	2004-2021	HEGIFTOM	N	N
De Bilt	52.1	5.18	862	2004-2020	HEGIFTOM	Y	Y
Valentia	51.94	-10.25	460	2004-2020	WOUDC	Y	N
Uccle	50.8	4.35	2348	2004-2020	HEGIFTOM	Y	Y
Praha	50.01	14.45	794	2004-2021	WOUDC	N	N
Kelowna**	49.93	-119.4	673	2004-2017	HEGIFTOM	N	Y
Hohenpeissenberg	47.8	11.02	2116	2004-2021	WOUDC	Y	Y
Payerne	46.49	6.57	2528	2004-2020	HEGIFTOM	N	Y
Haute Provence	43.94	5.71	800	2004-2021	NDACC	Y	Y
Yarmouth**	43.87	-66.11	754	2004-2021	HEGIFTOM	N	Y
Sapporo	43.06	141.33	387	2004-2018	WOUDC	Y	N
Trinidad Head	40.8	-124.16	913	2004-2022	NOAA	N	Y
Madrid	40.47	-3.58	775	2004-2021	HEGIFTOM	Y	Y
Boulder	40	-105.25	992	2004-2022	NOAA	Y	Y
Wallops Island	37.93	-75.48	850	2004-2020	SHADOZ	Y	Y
Tateno	36.06	140.13	516	2004-2021	WOUDC	Y	N
Huntsville	34.72	-86.64	777	2004-2020	NOAA	N	Y
Idabel	33.9	-94.75	149	2004-2016	TOPP	N	N
Houston	29.72	-95.34	505	2004-2017	TOPP	N	N
Izaña	28.3	-16.48	745	2004-2020	HEGIFTOM	Y	Y

Naha	26.21	127.69	419	2004-2018	WOUDC	Y	N
Hong Kong	22.31	114.17	776	2004-2020	WOUDC	Y	N
Hanoi	21.01	105.8	337	2004-2020	SHADOZ	Y	Y
Hilo*	19.43	-155.04	839	2004-2021	SHADOZ	Y (Mauna Loa)	Y
Costa Rica*	9.94	-84.04	659	2004-2021	SHADOZ	N	Y
Paramaribo	5.8	-55.21	608	2004-2021	HEGIFTOM	Y	Y
Kuala Lumpur	2.73	101.27	318	2004-2021	SHADOZ	N	Y
Quito	-0.2	-78.44	43	2004-2020	USFQ	N	N
San Cristobal*	-0.92	-89.62	176	2004-2016	SHADOZ	N	Y
Nairobi*	-1.27	36.8	641	2004-2019	SHADOZ	Y	Y
Natal*	-5.42	-35.38	472	2004-2021	SHADOZ	Y	Y
Watukosek	-7.5	112.6	124	2004-2013	SHADOZ	N	Y
Ascension*	-7.58	-14.24	490	2004-2021	SHADOZ	N	Y
Samoa*	-14.23	-170.56	568	2004-2021	SHADOZ	Y	Y
Fiji*	-18.13	178.4	236	2004-2021	SHADOZ	N	Y
Reunion	-21.06	55.48	553	2004-2020	SHADOZ	Y	Y
Irene	-25.9	28.22	233	2004-2020	SHADOZ	Y	Y
Broadmeadows	-37.69	144.95	790	2004-2020	WOUDC	Y	N
Lauder	-45	169.68	794	2004-2021	HEGIFTOM	Y	Y
Macquarie	-54.5	158.95	794	2004-2020	WOUDC	Y	N
Marambio	-64.24	-56.62	882	2004-2019	WOUDC	Y	N
Dumont d'Urville	-66.67	140	363	2004-2019	NDACC	Y	N
Davis	-68.58	77.97	473	2004-2019	WOUDC	N	N
Syowa	-69	39.58	529	2004-2021	WOUDC	Y	N
Neumayer	-70.62	-8.37	1186	2004-2021	NDACC	N	N
McMurdo	-77.85	166.67	174	2004-2010	NDACC	Y	Y
Belgrano	-77.87	-34.62	97	2004-2020	NDACC	Y	N
South Pole	-90	-169	984	2004-2021	NOAA	Y	Y
Total Profiles:			42042				
* Denotes the 14 S20 TCO dropoff stations							
** Kelowna and Yarmouth data corrected since S20 publication							
NOAA: ftp://ftp.gml.noaa.gov/data/ozwv/Ozonesonde/							
HEGIFTOM: http://hegiftom.meteo.be							
USFQ: https://observaciones-ia.usfq.edu.ec/							
NDACC: https://www-air.larc.nasa.gov/missions/ndacc/data.html							
WOUDC: https://woudc.org/data/explore.php?lang=en							
SHADOZ: https://tropo.gsfc.nasa.gov/shadoz/Archive.html							
TOPP: http://www.ruf.rice.edu/~ozone/							

Table 2. Additional metadata for the 60 global ozonesonde stations used in this study including the primary ozonesonde type and SST used. The farthest right column indicates the average EnSci ozonesonde percentage TCO change relative to OMI after EnSci S/N 25250. The average EnSci ozonesonde TCO change relative to OMI pre- and post-EnSci S/N 25250 considering *all* stations is -1.8%.

Station	Ozonesonde Type	SST Type	OMI% Change (25250)**
Alert*	EnSci, now SPC	1.0	0.1
Eureka*	EnSci, now SPC	1.0	-1
Ny-Ålesund	SPC	1.0	N/A
Thule	EnSci	0.5	N/A
Resolute	EnSci, now SPC	1.0	-2.9
Summit	EnSci	0.5	-1.2
Scoresbysund	EnSci	1.0	-5.6
Sodankyla	EnSci	0.5	-2.6
Lerwick	SPC	1.0	N/A
Churchill*	EnSci, now SPC	1.0	-5.8
Edmonton*	EnSci, now SPC	1.0	-2.2
Goose Bay	EnSci, now SPC	1.0	-1.1
Legionowo	SPC	1.0	N/A
De Bilt	SPC	1.0	N/A
Valentia	SPC	1.0	N/A
Uccle	EnSci	0.5	-0.9
Praha	SPC	1.0	N/A
Kelowna*	EnSci	1.0	-1.1
Hohenpeissenberg	Brewer-Mast	N/A	N/A
Payerne	EnSci	0.5	-1.3
Haute Provence	EnSci	1.0	N/A
Yarmouth*	EnSci, now SPC	1.0	-3.2
Sapporo	EnSci	0.5	0.1
Trinidad Head	EnSci	0.1	-1.2
Madrid	SPC	1.0	N/A
Boulder	EnSci	0.1	-1.5
Wallops Island	SPC	1.0	N/A
Tateno	EnSci	0.5	-1
Huntsville	EnSci	0.1	-2.5
Idabel	EnSci	0.5	-3.3
Houston	EnSci	0.5	-1.4
Izaña	SPC	1.0	N/A
Naha	EnSci	0.5	1
Hong Kong	SPC	1.0	N/A
Hanoi	EnSci	0.5	-1.3

Hilo*	EnSci	0.1	-2.8
Costa Rica*	EnSci	0.1	-5.6
Paramaribo	SPC	1.0	N/A
Kuala Lumpur	EnSci	0.5	N/A
Quito	EnSci	0.1	N/A
San Cristobal*	EnSci	0.1	N/A
Nairobi*	EnSci	0.5	-2
Natal*	SPC	1.0	N/A
Watukosek	EnSci	2.0	N/A
Ascension*	EnSci	0.5	N/A
Samoa*	EnSci	0.1	-3.6
Fiji*	EnSci	0.1	-4.4
Reunion	EnSci	0.5	-0.9
Irene	SPC	1.0	N/A
Broadmeadows	SPC	1.0	N/A
Lauder	EnSci	0.5	-2.6
Macquarie	SPC	1.0	N/A
Marambio	EnSci	0.5	-0.2
Dumont d'Urville	EnSci	0.5	N/A
Davis	SPC	1.0	N/A
Syowa	EnSci	0.5	1
Neumayer	SPC	1.0	N/A
McMurdo	EnSci	0.5	N/A
Belgrano	SPC	1.0	N/A
South Pole	EnSci	0.1	0
		Average Change:	-1.8
* Denotes the 14 S20 TCO dropoff stations			
** Requires minimum of 25 valid pre- and 25 valid post-EnSci 25250 serial number OMI TCO comparisons (otherwise marked N/A). Statistics consider only EnSci ozonesondes			

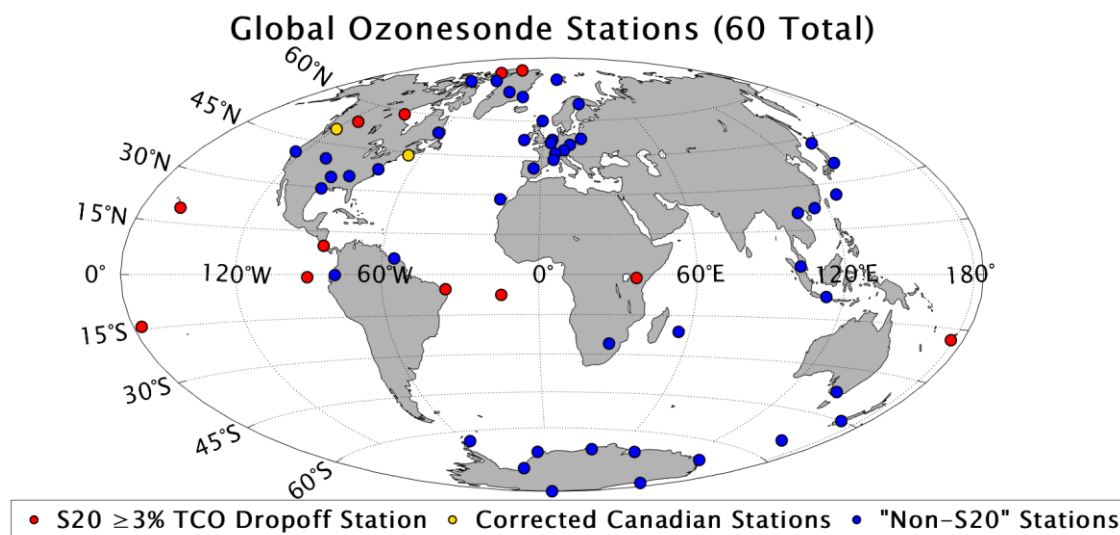


Figure 1. Map of the 60 global ozonesonde stations used in this study. All stations except Hohenpeissenberg (Brewer-Mast type) currently launch ECC ozonesondes. Stations (12 total) identified as having a $\geq 3\%$ TCO drop relative to OMI in S20 are shown as red dots, and the two Canadian stations (Kelowna and Yarmouth; see **Figure S2**) with corrected data for this study are shown as orange dots. Those two stations are still grouped with the “S20” stations for this analysis. All other stations (“Non-S20”; 46 total) are shown as blue dots.

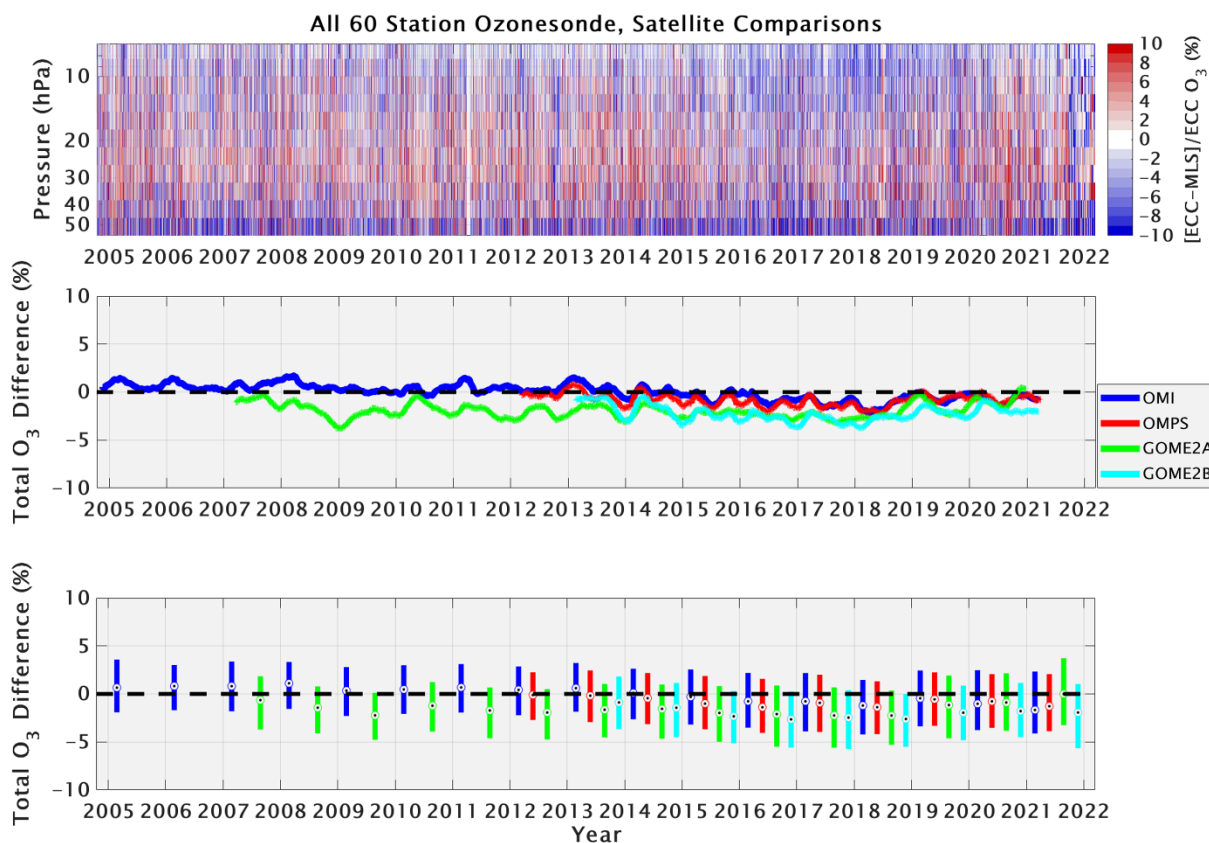


Figure 2. Coincident ozonesonde and satellite comparisons in percent difference for all 60 stations used in this study. *Top*: Time series of comparisons among all ozonesonde and MLS O_3 profiles ($[ECC-MLS]/ECC$). Red or blue colors indicate where the ozonesonde ozone is greater or less than MLS. *Middle*: Ozonesonde and satellite TCO comparisons in percent difference ($[ECC-satellite]/ECC$) for OMI (blue), OMPS (red), GOME-2A (green), and GOME-2B (cyan). The lines corresponding to each TCO satellite instrument indicate 500-ozonesonde centered, moving averages. No average lines are plotted for the first 250 and last 250 comparisons. *Bottom*: Ozonesonde and satellite TCO comparison statistics in percent difference for each individual year from 2005-2021. Bars represent the 25th to 75th percentile, with the dots representing the median comparison.

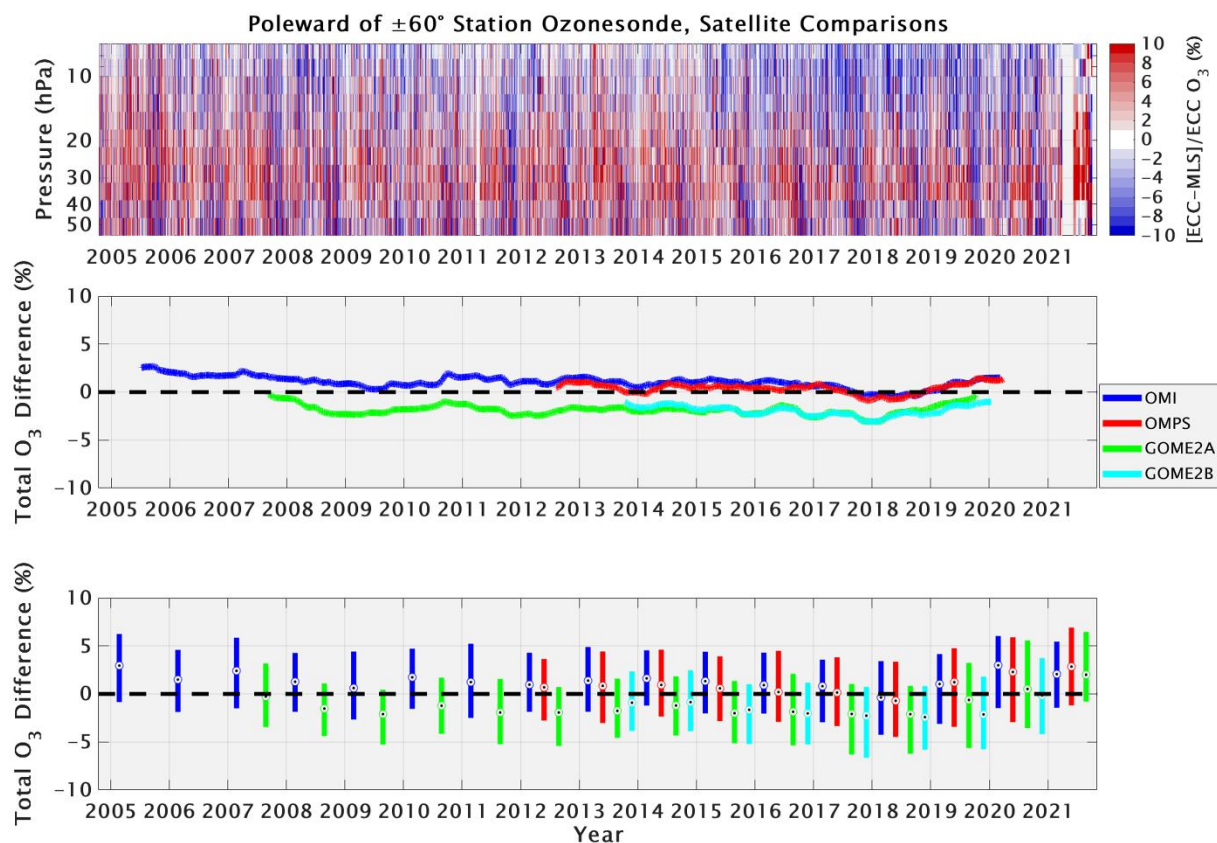


Figure 3. As in Figure 2, but for ozonesonde stations poleward of 60° latitude in both hemispheres.

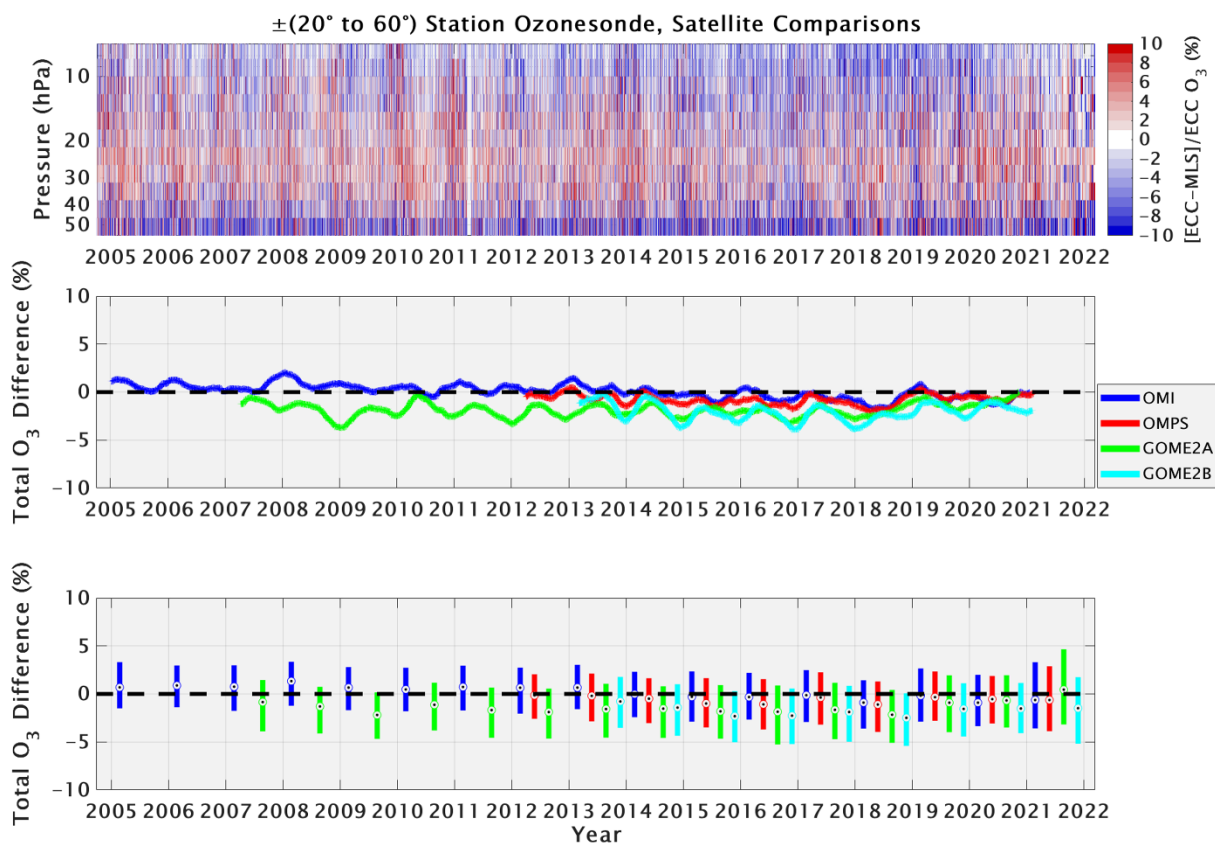


Figure 4. As in Figure 2, but for ozonesonde stations within $\pm(20 \text{ to } 60)^\circ$ latitude (i.e., “midlatitudes” in both hemispheres).

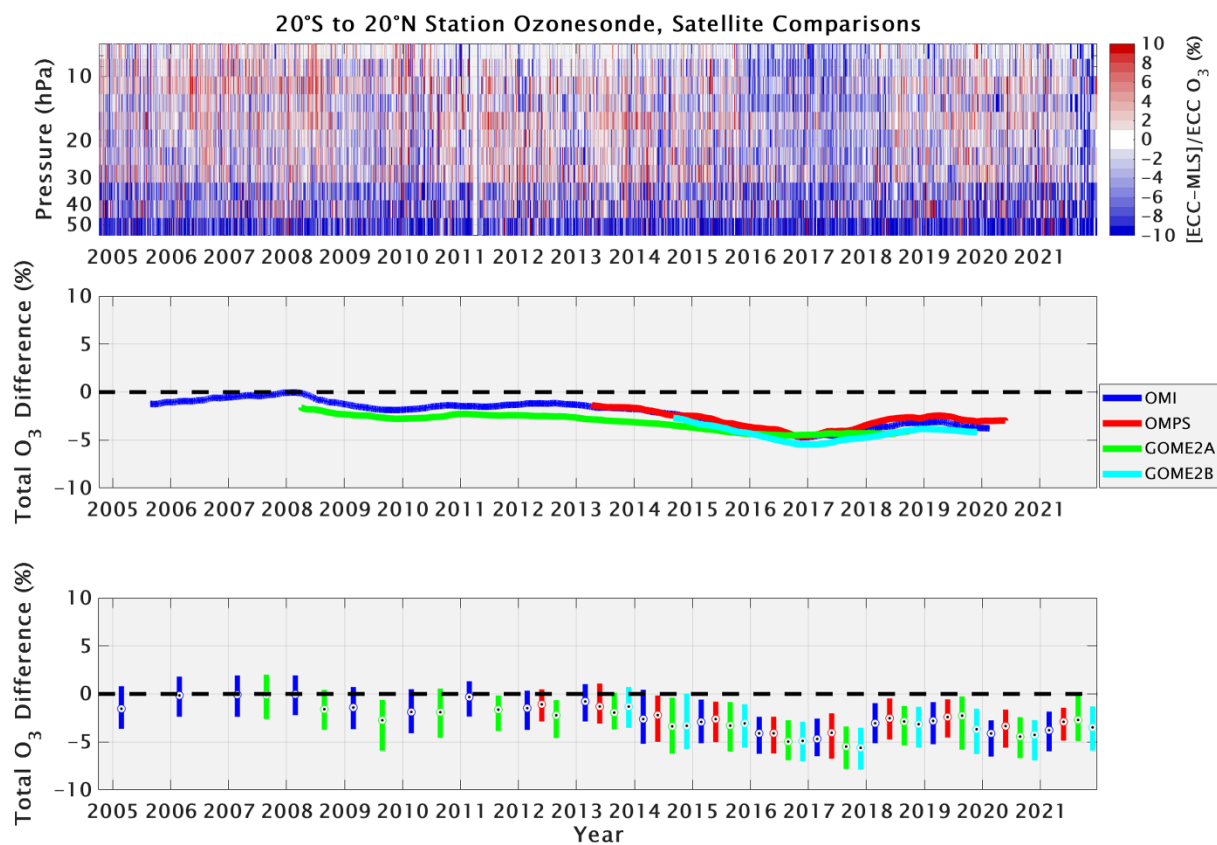


Figure 5. As in Figure 2, but for stations within 20° latitude of the equator.

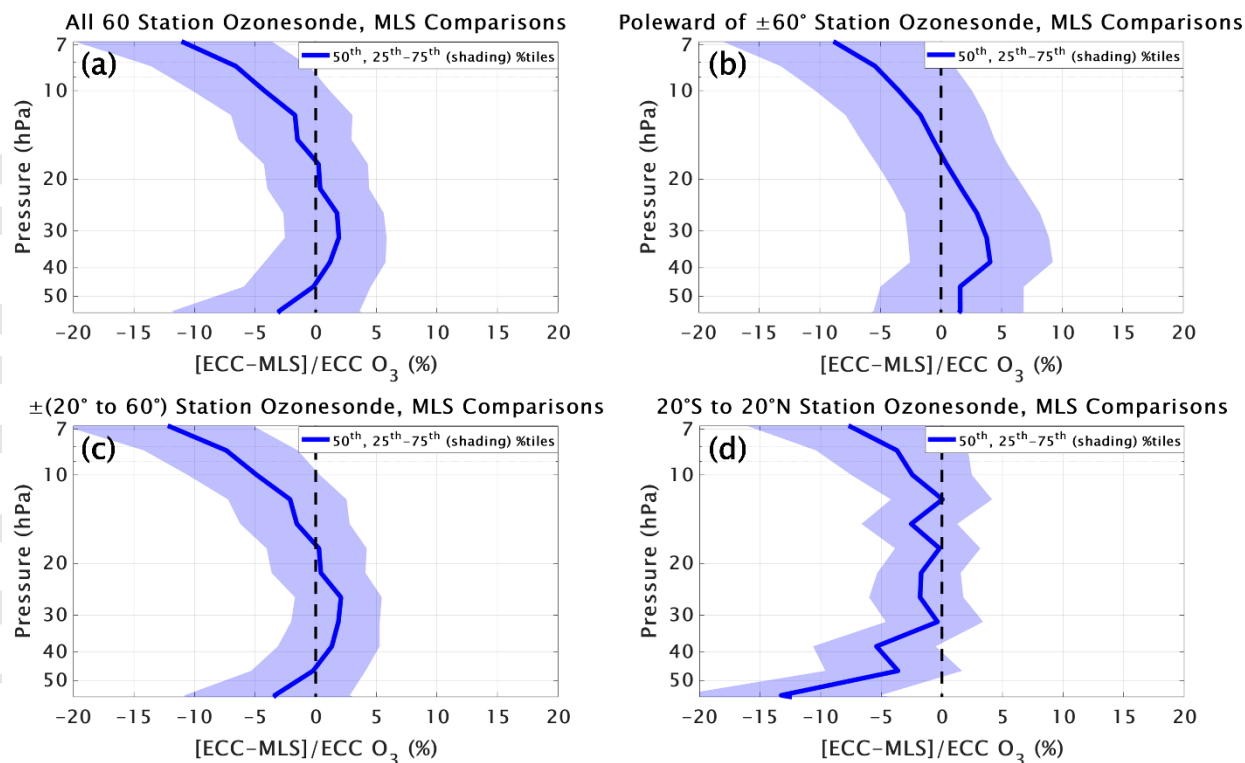


Figure 6. Comparisons of all coincident ozonesonde and Aura MLS ozone profiles in percent difference for the four latitude bands (a-d) referred to in Figures 2 through 5. The shading represents the 25th to 75th percentile, with the thick lines indicating the median (50th percentile) difference.

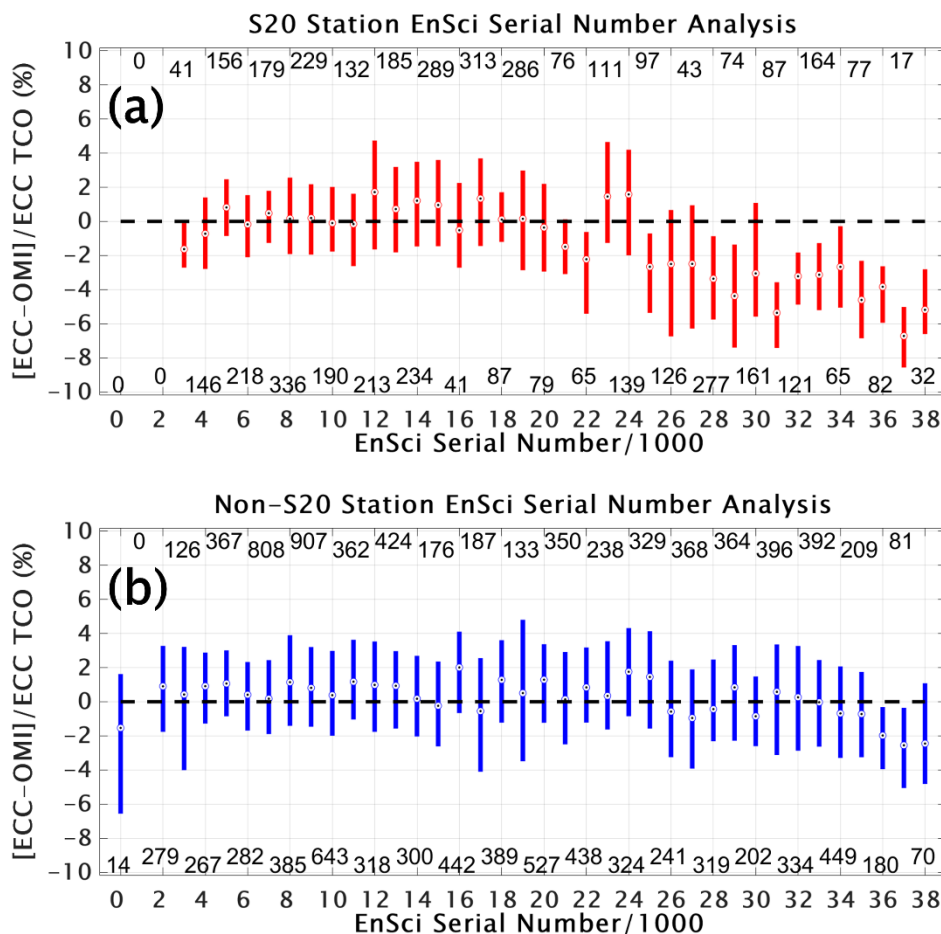


Figure 7. Comparisons of ECC ozonesonde TCO with OMI in percent difference for (a) all EnSci ozonesondes at the 14 S20 TCO dropoff stations, (b) all EnSci ozonesondes launched at the other 46 global stations in this study (note that some stations have not launched EnSci ECCs). EnSci S/Ns are grouped into bins of 1000 (26 = 26000 to 26999) for analysis. The bars show the 25th to 75th percentiles for each bin, with the dots representing the median value. The total number of valid ozonesonde/OMI comparisons for each bin are shown by the numbers along the top and bottom, aligned with the bars.

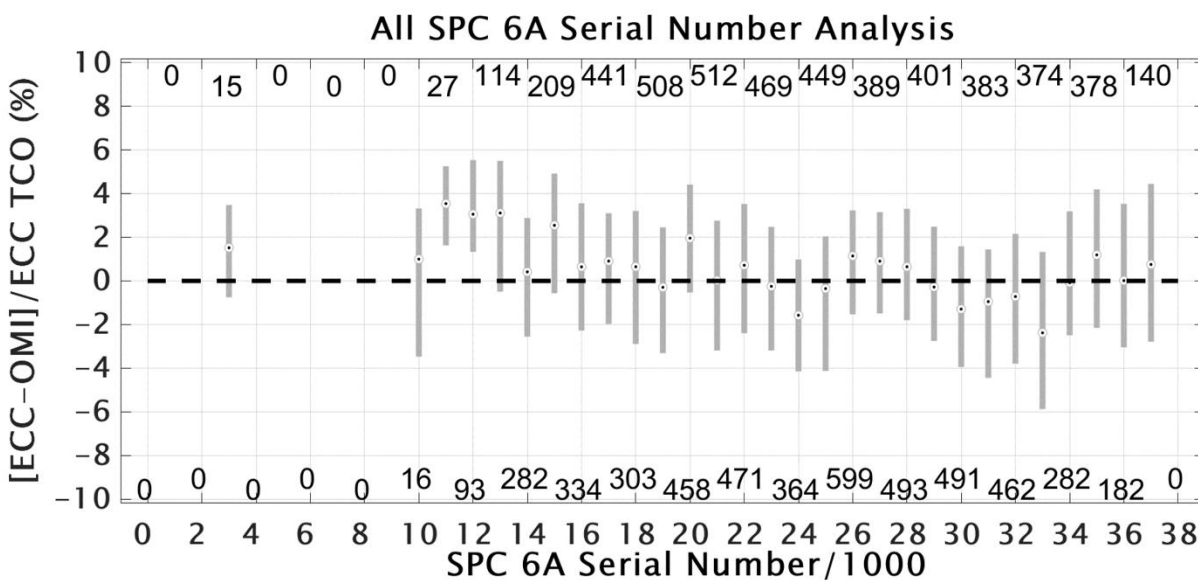


Figure 8. As in Figure 7, but for all SPC 6A ozonesondes launched at any of the 60 stations. Note that the similar S/Ns for EnSci and SPC 6A are a coincidence, and not all stations have launched SPC 6A ECCs.

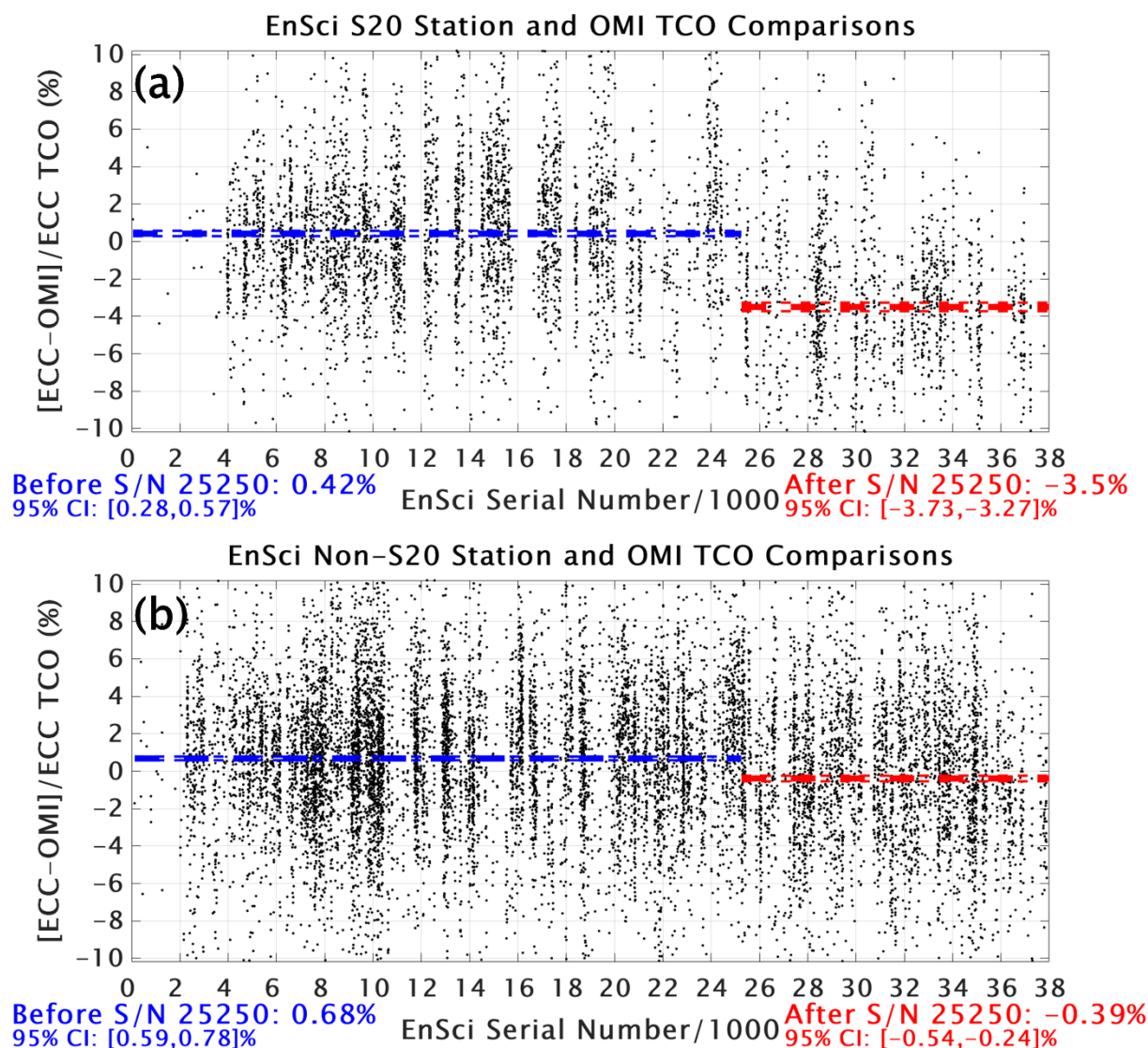


Figure 9. Comparisons in percent difference between ozonesonde and OMI TCO for all 14 S20 station (a) and all non-S20 station (b) EnSci S/Ns (all S/Ns are shown). The thick blue dashed line indicates the mean value for S/Ns prior to 25250, and the thick red dashed line indicates the mean value after S/N 25250. The mean values and their 95% confidence intervals (CI) are shown in text below both figures and the 95% CIs are indicated by the thin dashed lines.

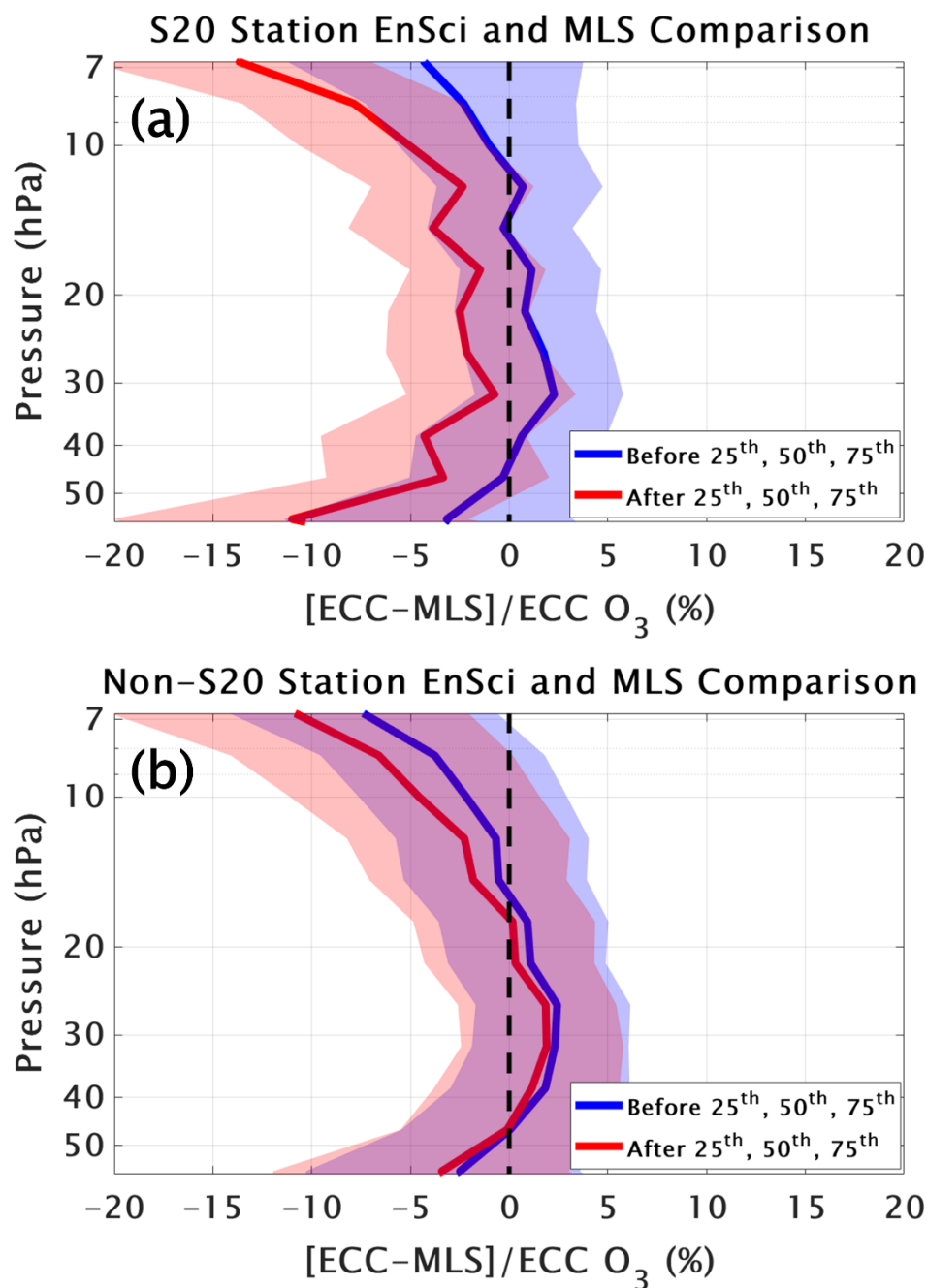


Figure 10. As in Figure 6, but here the comparisons are for EnSci ozonesondes only at the (a) 14 S20 stations and (b) non-S20 stations. The comparisons with Aura MLS ozone are shown for EnSci S/Ns prior to 25250 (blue) and after S/N 25250 (red). The shading represents the 25th to 75th percentile, with the median (50th percentile) difference shown by the solid lines.